Journal of proteome research

Article

pubs.acs.org/jpr

Characterization of 14-3-3 Isoforms Expressed in the *Echinococcus granulosus* Pathogenic Larval Stage

Aline Teichmann,[†,∥] Daiani M. Vargas,[†,∥] Karina M. Monteiro,[†] Bruna V. Meneghetti,[†] Cristine S. Dutra,[†] Rodolfo Paredes,[‡] Norbel Galanti,[§] Arnaldo Zaha,[†] and Henrique B. Ferreira*[,†]

[†]Laboratório de Genômica Estrutural e Funcional and Laboratório de Biologia Molecular de Cestódeos, Centro de Biotecnologia, Universidade Federal do Rio Grande do Sul (UFRGS), 91501-970 Porto Alegre, RS, Brazil

[‡]Escuela de Medicina Veterinaria, Facultad de Ecologia y Recursos Naturales, Universidad Andrés Bello, 8370251 Santiago, Chile

[§]Programa de Biología Celular y Molecular, Instituto de Ciencias Biomédicas, Facultad de Medicina, Universidad de Chile, 8389100 Santiago, Chile

Supporting Information

ABSTRACT: The 14-3-3 protein family of eukaryotic regulators was studied in *Echinococcus granulosus*, the causative agent of cystic hydatid disease. These proteins mediate important cellular processes in eukaryotes and are expected to play important roles in parasite biology. Six isoforms of *E. granulosus* 14-3-3 genes and proteins (Eg14-3-3.1−6) were analyzed, and their phylogenetic relationships were established with *bona fide* 14-3-3 orthologous proteins from eukaryotic species. Eg14-3-3 isoforms with previous evidence of expression (Eg14-3-3.1−4) in *E. granulosus* pathogenic larval stage (metacestode) were cloned, and recombinant proteins were used for functional studies. These protein isoforms were detected in different components of *E. granulosus* metacestode, including interface components with the host. The roles that are played by Eg14-3-3 proteins in parasite biology were inferred from the repertoires of interacting proteins with each isoform, as assessed by gel overlay, cross-linking, and affinity chromatography assays. A total of 95 Eg14-3-3 protein ligands were identified by mass spectrometry. Eg14-3-3 isoforms have shared partners (44 proteins), indicating some overlapping functions; however, they also bind exclusive partners (51 proteins), suggesting Eg14-3-3 functional specialization. These ligand repertoires indicate the involvement of Eg14-3-3 proteins in multiple biochemical pathways in the *E. granulosus* metacestode and note some degree of isoform specialization.

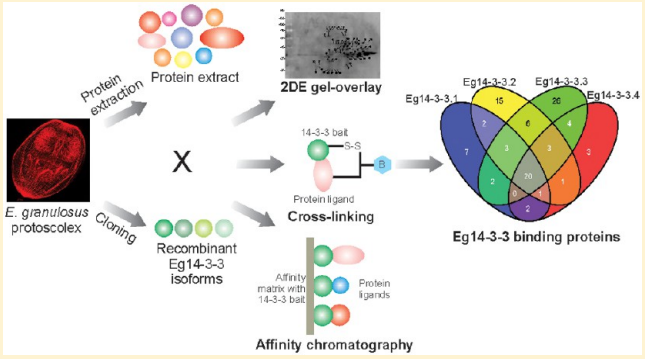

KEYWORDS: *14-3-3 proteins, Echinococcus granulosus, protein−protein interactions, host−parasite interactions*

INTRODUCTION

Hydatid disease is a parasitic infection that is caused by the larval stage of tapeworms of the genus *Echinococcus*. *Echinococcus granulosus* sensu lato (s.l.), a complex of four cryptic species with worldwide distribution, includes important members of the genus due to its infectivity to both human and animal hosts.[1] *Echinococcus granulosus* sensu stricto (s.s.), from now on referred to as *E. granulosus*, is the most prevalent species of the *E. granulosus* s.l. complex in South America and is responsible for most human echinococcal infections in Brazil.[2−4]

The *E. granulosus* pathogenic larval form (metacestode) is a two-layered unilocular cyst.[5] The cyst wall (CW) is formed by an inner layer called the germinal layer (GL) and an outer layer called the laminated layer (LL). The GL is responsible for the formation of brood capsules and preadults (protoscoleces, PSC). The GL also produces the LL, which is a thick, acellular, carbohydrate-rich, and specialized extracellular matrix. *E. granulosus* metacestodes are filled with the so-called hydatid fluid, which contains excretory−secretory products from both the GL and PSC, along with host proteins.[6]

E. granulosus metacestodes cause chronic infection in suitable intermediate hosts, being able to grow and remain viable and fertile (capable of producing protoscoleces) for long periods of time (up to years).[5] During this time, there is an intense cross-talk between parasite and host, with an exchange of proteins and other molecules. Host−parasite interactions are assumed to trigger important signaling pathways in both parasite and host cells, which are determinants of the infection outcome and parasite development.[6] In this scenario, 14-3-3 proteins, which are ubiquitous eukaryotic cell regulators,[7−9] are expected to mediate important parasite cellular functions, depending on their interactions with different protein counterparts.

The 14-3-3 proteins are highly conserved and can perform a wide range of cellular functions by interacting with a ligand

Received: September 29, 2014
Published: March 9, 2015

DOI: 10.1021/pr5010136
J. Proteome Res. 2015, 14, 1700−1715

repertoire that exceeds 300 interaction partners in different organisms.[10−12] Structurally, 14-3-3 are small (~30 kDa), acidic proteins that form both homo- and heterodimers, which can bind either to phosphoserine/phosphothreonine residues or to sequence-specific, nonphosphorylated motifs of protein partners.[10] The 14-3-3 proposed mechanisms of action include the modification of activity of the bound ligands, changes in the association of the bound ligands with other cellular components, and the altered intracellular destination of 14-3-3 bound cargo.[13]

The number of different 14-3-3 isoforms varies from species to species. This number can be as low as two, such as in yeast, *Caenorhabditis elegans*, and *Drosophila melanogaster*, to as high as seven in mammals or 12 in *Arabidopsis*.[13] In helminth parasites, 14-3-3 proteins have been identified at the host−parasite interface[14] and described as differentially expressed between parasite stages[15] and as potential diagnostic or vaccinal antigens.[16,17] For *E. granulosus*, six 14-3-3 protein-encoding genes were annotated in the genome sequences.[15,18] The expression of four of these 14-3-3 isoforms in distinct parasite life stages, metacestode components, and in excretion/secretion products of protoscoleces has been detected by transcriptomic[15,18,19] and proteomic studies.[7,9] Immunohistochemical studies of *E. granulosus* adult worm also showed an association of 14-3-3 proteins with the outer apical area (rostellum) and rostellar gland secretion, suggesting roles in parasite adhesion and nutrition.[20] Despite this evidence that the 14-3-3 protein family plays important roles in *E. granulosus* development, virtually no information is available on the cellular processes that are regulated by these proteins.

In the present study, we revised and compared the exon−intron organization of *E. granulosus* 14-3-3 genes (*Eg14-3-3*). The deduced amino acid sequences were used to provide three-dimensional molecular models and to establish the phylogenetic relationships of the Eg14-3-3 with 14-3-3 proteins of a wide range of organisms, including parasites and model organisms. To gather evidence for Eg14-3-3 functions in parasite biology, especially during the infection of the intermediate host, we also investigated the repertoires of interacting proteins with each of the four Eg14-3-3 isoforms that are expressed during the *E. granulosus* metacestode stage. Three independent methods demonstrated that, along with several shared protein interactions, each Eg14-3-3 isoform has a set of exclusive ligands, which is suggestive of functional specialization. The identified sets of protein ligands indicate the involvement of 14-3-3 proteins in several *E. granulosus* cellular functions, such as energy production, carbohydrate metabolism, and intracellular trafficking. The implications of Eg14-3-3 protein interactions and its inferred roles in parasite survival and growth during host infection are discussed.

MATERIALS AND METHODS

Parasite Material

E. granulosus hydatid cysts were obtained from the lungs and livers of naturally infected bovines from a commercial slaughterhouse (São Leopoldo, Rio Grande do Sul, Brazil). The hydatid cyst fluid (HCF) was aseptically aspirated and 10-fold concentrated by lyophilization. The GL was separated from the laminated layer using a tissue scraper. Protoscoleces (PSC) were washed three times in phosphate buffered saline (PBS). Parasite genotyping, for confirmation of the G1 haplotype for *E. granulosus* s.s., was performed as described by Balbinotti et al.[2]

Nucleotide and Amino Acid Sequences and Phylogenetic Analyses

The *E. granulosus* genome sequences that were used in this work were obtained from GeneDB (www.genedb.org). The six annotated *E. granulosus* 14-3-3 genes (EgrG_001192500, EgrG_000231300, EgrG_000364000, EgrG_001060100, EgrG_000789700, and EgrG_000314100), here referred to as *Eg14-3-3.1−6*, respectively, were analyzed with the GeneMark-E,[21] Fgenesh,[22] and GeneScan[23] algorithms to confirm the exon−intron structures and coding DNA sequences (CDSs). The CDS translations and protein molecular mass and isoelectric point predictions were performed using tools that were available on the ExPASy Web site (http://expasy.org/). The deduced amino acid sequences were aligned using ClustalW2 (http://www.ebi.ac.uk/Tools/msa/clustalw2/).

Forty-eight orthologous 14-3-3 protein sequences from parasites and model organisms were recovered from the GeneDB and NCBI (http://www.ncbi.nlm.nih.gov/) databases using the BLAST tool and Eg14-3-3 sequences as queries. Phylogenetic analyses were performed by the neighbor-joining[24] methods using MEGA6.[25] The percentages of replicate trees in which the associated taxa clustered together in the bootstrap test (1000 replicates) are shown next to the branches. The evolutionary distances were computed using the p-distance method. All of the ambiguous positions were removed for each sequence pair. There were a total of 328 positions in the final data set.

Molecular Modeling of the Eg14-3-3 Isoforms

Tridimensional (3D) molecular models of Eg14-3-3 isoforms were built by comparative modeling. The search for templates and the generation of molecular models were conducted as previously described.[26] The templates that were used for Eg14-3-3 modeling were from *Homo sapiens* (PDB code: 2BR9)[27] for Eg14-3-3.1, *Nicotiana tabacum* (PDB code: 1O9C)[28] for Eg14-3-3.2, *Bos taurus* (PDB codes: 2V7D and 1A38)[29,30] for Eg14-3-3.3 and Eg14-3-3.4, respectively, *H. sapiens* (PDB code: 3UAL)[31] for Eg14-3-3.5, and *Cryptosporidium parvum* (PDB code: 2NPM)[32] for Eg14-3-3.6. Alignments between Eg14-3-3 isoforms and the templates were used to generate Eg14-3-3 3D structures using Modeller version 9.8.[33] The visualization and manipulation of the molecular images were performed with PyMOL version 1.3 (www.pymol.org). The final models were evaluated with PROSA-web (https://prosa.services.came.sbg.ac.at/prosa.php), PROCHECK (http://www.ebi.ac.uk/thornton-srv/software/PROCHECK/), TM-score (http://zhanglab.ccmb.med.umich.edu/TM-score/), Swiss-pdb Viewer (http://spdbv.vital-it.ch/), and Qmean Server (http://swissmodel.expasy.org/qmean/cgi/index.cgi).

RNA Extraction, cDNA Synthesis, and Cloning

E. granulosus PSC RNA extraction, cDNA synthesis, and cloning were carried out essentially as described by Lorenzatto et al.[34] The coding sequences of the Eg14-3-3 isoforms were amplified by PCR with gene-specific primers for Eg14-3-3.1 (5′-TTGGTCGTTATGTCTTCTCTCAGT-3′ and 5′-CTCCGACATTTCTTCATTTA-3′), Eg14-3-3.2 (5′-ATGGCTACGAAAAGTCCTA-3′ and 5′-CTAATCCCGCTTGTCACC-3′), Eg14-3-3.3 (5′-ATGGCAGCTATTACCTCTTG-3′ and 5′-TTAGGAGTCGGTCTCACATT-3′), and Eg14-3-3.4 (5′-ATGGCTGAGCTTCTGTCCAC-3′ and 5′-TTCAGCACCCTCGGTATT-3′). The gene-specific forward and reverse primers also included 24 nt recombination tags matching the cloning vector pGEX-TEV, with FrecI (5′-TATTTTCAGGG-

DOI: 10.1021/pr5010136
J. Proteome Res. 2015, 14, 1700−1715

AGAATTCCCGGGT-3′) and RrecI (5′-GCGAGGCAGAT-CGTCAGTCAGTCA-3′) respectively added to their 5′ ends. The PCR products were used as templates for a second amplification reaction with primers containing additional nucleotide sequences matching the cloning vector, namely, FrecII (5′-TGGTTCCGCGTGGATCTGAAAACCTGTA-TTTTCAGGGAGAATTCCCGGGT-3′) and RrecII (5′-GGTTTTCACCGTCATCACCGAAACGCGCGAGGCAG-ATCGTCAGTCAGTCA-3′). The *Eg14-3-3* CDSs (*Eg14-3-3.1*, 744 bp; *Eg14-3-3.2*, 768 bp; *Eg14-3-3.3*, 747 bp; and *Eg14-3-3.4*, 771 bp), which were tagged with 50 bp matching pGEX-TEV at their 5′ and 3′ ends, were cloned by *in vivo* homologous recombination.

Recombinant Protein Expression and Purification

Recombinant Eg14-3-3 isoforms were expressed using *Escherichia coli* strains Rosetta, BL21-CodonPlus-RP, and BL21-CodonPlus-RIL (Stratagene, USA). The expression of the recombinant proteins that were fused to glutathione S-transferase (GST) (1 L of culture) was induced with isopropyl β-D-1-thiogalactopyranoside (IPTG) to a final concentration of 0.1 mM at 37 or 20 °C for 3 or 18 h. After induction, the cells were harvested and lysed. GST fusion proteins were recovered from the soluble fraction by affinity chromatography in Glutathione Sepharose 4B (GE Healthcare, UK) followed by cleavage with TEV protease as previously described.[34] The purified proteins were analyzed by 12% SDS-PAGE, and the protein concentrations were measured using a Qubit quantitation fluorometer and Quant-iT reagents (Invitrogen, USA).

Immunoblots

Eg14-3-3 isoform-specific antisera were produced by rabbit immunization. Antisera production and antibody purification were carried out as previously described,[34] using 250 μg of each Eg14-3-3 recombinant protein per animal in each of the three performed immunizations. The experimental procedures were previously approved by the Ethical Committee of the Universidade Federal do Rio Grande do Sul (http://www.ufrgs.br/ceua/). For immunoblot assays, *E. granulosus* PSC and GL samples were homogenized in a glass Dounce tissue grinder with PBS containing 1 mM PMSF and 1% Triton X-100. The homogenates were centrifuged at 20 000*g* for 30 min at 4 °C to remove the insoluble fraction. The soluble proteins were quantified using a Qubit quantitation fluorometer and Quant-iT reagents (Invitrogen). The protein samples were resolved by 12% SDS-PAGE and transferred to PVDF membranes (Hybond, GE Healthcare). The membranes were blocked for 16 h with 5% nonfat dry milk in PBS-T (PBS containing 0.1% Tween-20) and then incubated with specific anti-14-3-3 isoform rabbit polyclonal antibodies at a 1:20000 (v/v) dilution for 1 h and 30 min. After four washes with PBS-T, the membranes were incubated with a goat anti-rabbit IgG−horseradish peroxidase (ECL, GE Healthcare) at a 1:9000 (v/v) dilution for 1 h. Antigen−antibody reactions were detected with the ECL Plus kit (GE Healthcare) and imaged using the VersaDoc imaging system (Bio-Rad, USA). Recombinant Eg14-3-3 proteins (~50 ng) were used to assess the antisera specificity.

Immunofluorescence

E. granulosus PSC and CW tissues were prepared as described by Paredes et al.[35] Paraffin-embedded sections (5 μm thick) were blocked with 1% bovine serum albumin (BSA, Sigma-Aldrich, USA) and 0.05% Tween in PBS for 1 h at 37 °C. The sections were then incubated in a humid chamber for 1 h at 37 °C with isoform-specific anti-Eg14-3-3 purified IgG that was diluted 1:50 v/v in blocking solution. After three washes with PBS, sections were incubated in a humid chamber for 1 h at 37 °C with goat anti-rabbit IgG conjugated with Alexa Fluor 488 (Invitrogen) that was diluted 1:100 v/v in blocking solution. The sections were then incubated with 50 μM 4′,6-diamidino-2-phenylindole (DAPI) for 20 min at 37 °C and mounted with Fluoromount.

Whole-mount specimens were prepared as described by Koziol et al.[36] with some modifications. *E. granulosus* PSC were fixed with 4% paraformaldehyde for 30 min and washed three times (10 min each) with PBS/0.3% Triton X-100 (PBS-Triton). The sample permeabilization was achieved by a 5 min treatment with 20 μg/mL proteinase K (Fermentas, USA) in PBS−Triton, followed by refixation with 4% paraformaldehyde for 10 min at room temperature. The samples were then washed three times with PBS−Triton and blocked for 2 h in PBS−Triton with 3% BSA. Incubation with isoform-specific anti-Eg14-3-3 purified IgG antibodies diluted 1:50 v/v in PBS−Triton with 3% BSA was carried out overnight at 4 °C. The samples were then washed six times with PBS−Triton for 10 min each and incubated for 1 h at 37 °C with goat anti-rabbit IgG that was conjugated with Alexa Fluor 488 (Invitrogen) and diluted 1:100 v/v in PBS−Triton. Finally, the samples were washed six times with PBS−Triton for 10 min each, co-stained with 50 μM DAPI and Phalloidin Alexa Fluor 594 (Sigma-Aldrich) for 20 min at 37 °C, and mounted with Fluoromount. Sections and whole-mount specimens were observed under the confocal microscope (Olympus FluoView 1000). The images were digitally captured and processed using the Olympus FluoView, version 2.1c, and the Olympus FluoView, version 3.0, Viewer software.

Two-Dimensional Gel Overlay

Two-dimensional (2D) gel electrophoresis and gel overlay experiments were performed as described by Monteiro et al.[7] and Meek et al.,[37] respectively, with modifications. *E. granulosus* PSC were homogenized in a glass Dounce tissue grinder with 50 mM Tris-Cl, pH 7.5, 1% Triton X-100, 1 mM DTT, 1 mM PMSF, 1 mM Na_3VO_4, 50 mM NaF, 1.15 mM Na_2MoO_4, and 2 mM Mg-ATP. The homogenates were centrifuged at 20 000*g* for 30 min at 4 °C to remove the insoluble fraction. The soluble proteins were quantified by fluorimetry using a Qubit quantitation fluorometer and Quant-iT reagents (Invitrogen). The protein extracts (2 mg) were separated by 2D gel electrophoresis (20 × 20 cm, 12% SDS-PAGE gels) and electrotransferred to nitrocellulose membranes (Hybond, GE Healthcare) as described by Monteiro et al.[7] Then, the membranes were blocked for 16 h with 5% ECL blocking agent (GE Healthcare) and individually incubated for 2 h at 4 °C with recombinant Eg14-3-3 protein isoforms (1 μg/mL) that were previously biotinylated with the ECL protein biotinylation module (GE Healthcare). Protein−protein interactions were detected with streptavidin−horseradish peroxidase conjugate, followed by revelation with ECL reagents (GE Healthcare), and imaged using the VersaDoc imaging system (Bio-Rad). The images from the 2D gel electrophoresis and 2D gel overlay experiments were analyzed using PDQuest 8.0 software (Bio-Rad) for spot detection and matching. For Eg14-3-3-binding protein identification, reactive protein spots were manually excised from corresponding 2D gels and

DOI: 10.1021/pr5010136
J. Proteome Res. 2015, 14, 1700−1715

digested with trypsin according to Monteiro et al.[7] The resulting peptides were analyzed by mass spectrometry, as described in the mass spectrometry section. A 2D gel overlay control experiment was performed with the GST protein tagged with biotin. Specificity controls were carried out by one-dimensional gel overlay using biotinylated Eg14-3-3 recombinant proteins that were preincubated for 1 h with 0.016 mM or 0.1 mM of the competitor R18 peptide (CVPRDLSWLDLE-ANMCLP)[37] (Bachem, USA). All overlay experiments were performed in replicate, with each replicate containing a pool of PSC that was obtained from three to five different individuals (metacestodes). Higher than 90% of coincidence was observed between replicates for both gel and blotting spots.

Protein Cross-Linking

E. granulosus PSC proteins that interact with Eg14-3-3 recombinant isoforms were recovered by cross-linking using the Sulfo-SBED (sulfosuccinimidyl-2-[6-(biotinamido)-2-(*p*-azido-benzamido) hexanoamido] ethyl-1,3-dithiopropionate) biotin label transfer reagent (Pierce, USA) according to the manufacturer's instructions. Briefly, 1 mg of Eg14-3-3 recombinant isoforms was labeled with a 5-fold molar excess of Sulfo-SBED. Sulfo-SBED−Eg14-3-3 complexes were individually incubated with a PSC protein extract (5 mg, processed as described for two-dimensional gel overlay experiments) for 30 min at room temperature and for 15 min under UV irradiation that was produced by a Boitton UV lamp (365 nm, 6 W) at a distance of 5 cm. The complexes Eg14-3-3−Sulfo-SBED-interacting proteins were cleaved with DTT, and the biotin-labeled Eg14-3-3-interacting proteins were recovered by affinity chromatography using a monomeric avidin column (Pierce). The bound proteins were sequentially washed with five column volumes of each of the following buffers: PBS, PBS/0.1% Triton-X-100, PBS, 100 mM NaCl/0.05% SDS, 200 mM NaCl/0.05% SDS, and PBS. The biotinylated proteins were eluted from the resin with 2 mM biotin (Pierce). The protein extracts that were used for the cross-linking experiments were produced from a pool of PSC from five different individuals (metacestodes), which was necessary to provide the minimum amount of protein that was required to perform the experiments. This PSC pool was assumed to be representative of possible biological variations.

Eg14-3-3 Affinity Chromatography

Recombinant Eg14-3-3 proteins were individually coupled to an activated CH-Sepharose 4B (Sigma-Aldrich) following the manufacturer's instructions. The beads with immobilized Eg14-3-3 recombinant isoforms were separately incubated with an *E. granulosus* PSC protein extract (20 mg, processed as described for two-dimensional gel overlay experiments) for 16 h at 4 °C. Then, the resins were transferred to disposable chromatography columns (Bio-Rad) and washed with 10 bed volumes of low-salt wash buffer (50 mM Tris-HCl, pH 7.5, 150 mM NaCl, 1 mM DTT), followed by washes with 10 volumes of high-salt buffer (50 mM Tris-HCl, pH 7.5, 500 mM NaCl, 1 mM DTT). The Eg14-3-3-binding proteins were specifically eluted from the columns with 5 mL of 1 mM R18 peptide that was dissolved in high-salt buffer. The protein extracts that were used for the affinity chromatography experiments were produced from a pool of PSC from 20 different individuals (metacestodes), which was necessary to provide the minimum amount of protein that was required to perform the experiments. This PSC pool was assumed to be representative of possible biological variations.

Mass Spectrometry

Tryptic peptides from 2D gel electrophoresis protein spots were analyzed by MALDI-Q-TOF MS/MS (Waters, UK) as described by Monteiro et al.[7] The analyses were performed on a Waters Micromass Q-TOF Premier mass spectrometer that was equipped with a standard MALDI source (Waters). The MS spectra were recorded from 800 to 3000 m/z, with an automatic scan rate of 1 s and an interscan delay of 0.1 s. The MS/MS spectra for the five most intense ions were automatically acquired in data-dependent acquisition (DDA) mode, when the peak intensity increased to greater than a 30-count threshold. The CID collision energy was automatically set according to the m/z ratio of the precursor ion.

The Eg14-3-3-interacting proteins that were recovered by protein cross-linking and affinity chromatography were precipitated overnight at −20 °C with ice-cold 20% (w/v) trichloroacetic acid/acetone, and the protein pellet was resuspended in 8 M urea/25 mM NH_4HCO_3, pH 8.0. The samples were subjected to trypsin digestion and desalination as described by Monteiro et al.[7] The mass spectrometric analysis was performed using the nanoflow liquid chromatography-tandem mass spectrometry system (nLC−MS/MS) on an EASY-nLC system (Proxeon Biosystem, USA) that was connected to a LTQ Orbitrap Velos mass spectrometer (Thermo Fisher Scientific, USA) through a Proxeon nano-electrospray ion source. Two micrograms of peptides was separated with a 2−90% acetonitrile gradient in 0.1% formic acid using the analytical PicoFrit Column (C18, 20 cm × i.d. 75 μm, 5 μm particle size, New Objective, USA) at a flow of 300 nL/min for 65 min. The nanoelectrospray voltage was set to 2.2 kV, and the source temperature was 275 °C. The full-scan MS spectra (m/z 300−1600) were acquired in the Orbitrap analyzer after accumulation to a target value of 1×10^6. The resolution in the Orbitrap was set to $r = 60\,000$, and the 20 most intense peptide ions with charge states ≥ 2 were sequentially isolated to a target value of 20 000 and fragmented in the linear ion trap using low-energy CID (normalized collision energy of 35%). The signal threshold for triggering an MS/MS event was set to 1000 counts. Dynamic exclusion was enabled with an exclusion size list of 500, an exclusion duration of 60 s, and a repeat count of 1. An activation $q = 0.25$ and activation time of 10 ms were used.

Database Searching and Bioinformatics

The raw files were processed using Mascot Distiller version 2.4 to generate mgf files. For protein identification, MS/MS data were searched using Mascot software version 2.3.02 against a local *E. granulosus* database containing deduced amino acid sequences (10,445) from genome annotation as available on GeneDB. For MALDI-Q-TOF MS/MS, the following parameters were used: maximum of one missed cleavage, fixed carbamidomethyl alkylation of cysteines, variable oxidation of methionine, and 0.1 mass unit tolerance on parent and fragment ions. The significance threshold was set at $p < 0.05$, and only those peptides with individual ion scores above this significance threshold were considered for protein identification. For the LTQ Orbitrap Velos mass spectrometer, the search parameters consisted of carbamidomethylation as a fixed modification, oxidation of methionine as a variable modification, one trypsin missed cleavage, and a tolerance of 10 ppm for precursor and 1 Da for fragment ions. Scaffold, version 4.0.5, was used to validate the peptide and protein identifications. The peptide identifications were accepted if they could be

DOI: 10.1021/pr5010136
J. Proteome Res. 2015, 14, 1700−1715

established with >95% probability, as specified by the Peptide Prophet algorithm,[38] and protein identifications were accepted if they could be established at a >99% probability and contained at least two identified peptides.[39] Eukaryotic orthologous group (KOG)[40] annotations were assigned to identified proteins based on sequence similarity searches against the KOG annotated proteins using the $eggNOG_{4.0}$ tool (http://eggnog.embl.de/version_4.0.beta/).[41]

RESULTS AND DISCUSSION

Eg14-3-3 Genes and Encoded Proteins

The six *Eg14-3-3* genes were compared regarding their exon−intron structures and sequences. These genes contain three or four exons ranging in size from 33 to 384 bp that are separated by introns ranging in size from 29 to 190 bp (Figure S1). The *Eg14-3-3* genes encode Eg14-3-3 proteins with 211−256 aa and deduced molecular masses ranging from ∼24.3 to ∼29.4 kDa (Table S1). Eg14-3-3.5 is the smallest protein isoform due to its shorter N-terminal extension.

The sequence alignments of the Eg14-3-3 deduced amino acid sequences (Figure S2) shows identities/similarities ranging from 21−54% to 38−72%, respectively, between paralogs. The 14-3-3.5 isoform is the most divergent, with a 21%/38% overall identity/similarity between paralogs. Multiple sequence alignments were also performed between the Eg14-3-3 proteins and the 14-3-3 orthologous proteins from a wide range of eukaryotic species, including other helminthes and model organisms. This analysis revealed identities between ∼30 and 99% with other helminthes and between ∼30 and 50% with model organisms (Table S2).

To further explore the phylogenetic relationships of Eg14-3-3 proteins, we built a phylogenetic tree including the 48 ortholog sequences that were used in the alignments described above. This analysis demonstrated that Eg14-3-3 proteins, along with 14-3-3 proteins from other helminthes, form a group separate from that formed by 14-3-3 proteins from more complex organisms, such as *D. melanogaster*, *B. taurus*, and *H. sapiens* (Figure S3).

Eukaryotic 14-3-3 proteins are typically grouped into two distinct groups, one comprising the nonepsilon isoforms and another comprising the epsilon isoforms.[42] In our analysis, these groups were indeed observed for 14-3-3 proteins from more complex organisms, which formed a wide monophyletic group, including beta, alpha, zeta, delta, theta, eta, gamma, and sigma isoforms, apart from the other monophyletic group formed by epsilon isoforms.

Eg14-3-3.1−6 isoforms form another six monophyletic groups, along with their respective orthologs from related organisms, such as *Echinococcus multilocularis*, *Taenia solium*, and *Hymenolepis microstoma*. The Eg14-3-3.5 and Eg14-3-3.6 isoforms diverge not only from 14-3-3 proteins from more complex organisms but also from their paralogs. This indicates that the six-paralog configuration of the *Echinococcus* 14-3-3 family was established prior to the speciation events that separated *E. granulosus* and *E. multilocularis*.

Structural Modeling of Eg14-3-3 Isoforms

To gain insights into the structure of Eg14-3-3 proteins, we built 3D molecular models for the six isoforms, using the available ortholog templates with the highest identities/similarities with each of the studied isoforms. Quality assessments of the Eg14-3-3-built models indicated good overall accuracy and stereochemical properties (Table S3). The 3D models (Figure 1) indicate that the Eg14-3-3.1−4 isoforms have typical structural characteristics of *bona fide*

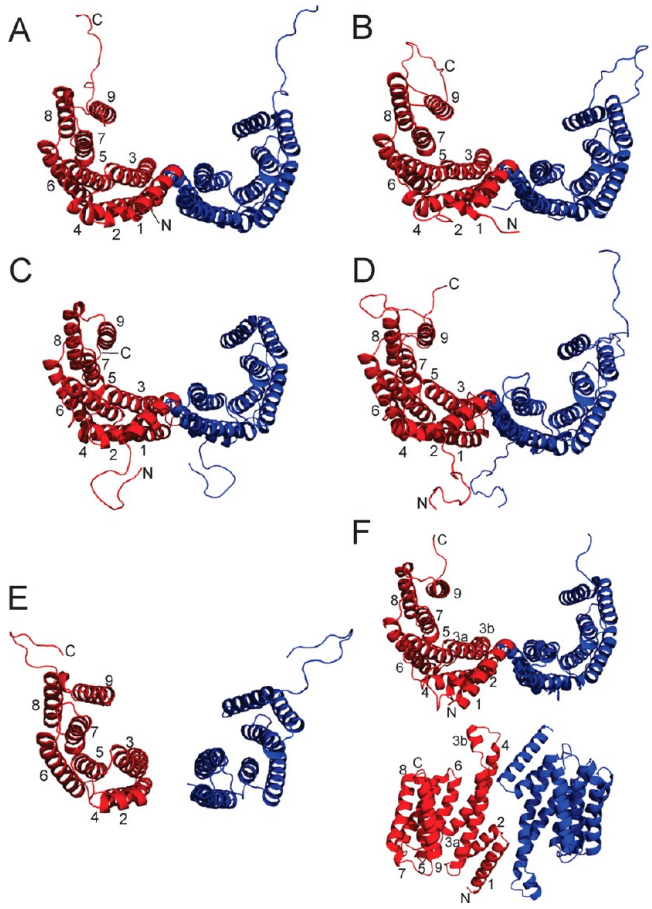

Figure 1. Modeled 3D structures of homodimers from (A) Eg14-3-3.1, (B) Eg14-3-3.2, (C) Eg14-3-3.3, (D) Eg14-3-3.4, (E) Eg14-3-3.5, and (F) Eg14-3-3.6 (in two views: the top one parallel to the helices axis and the bottom one perpendicular to this axis). The monomers are represented by different colors (red and blue), and the α-helices are indicated by numbers, according to the text.

eukaryotic 14-3-3 proteins, whereas Eg14-3-3.5 and Eg14-3-3.6 isoforms were more divergent.

In the Eg14-3-3.1−4 models (Figure 1A−D), each monomer consists of nine antiparallel α-helices (α1−9, indicated in Figures 1 and S2), forming an elongated bundle. On the other hand, the Eg14-3-3.5 and Eg14-3-3.6 models present elongated bundles formed by different α-helix configurations (Figure 1E,F), whereas Eg14-3-3.5 present eight α-helices, missing the first N-terminal (α1) helix (Figure 1E), and Eg14-3-3.6 presents a structure with the α3 helix split into two shorter α-helices (α3a−α3b, Figure 1F). In all Eg14-3-3 protein models, the N-terminal and C-terminal ends were not structured and presented different sizes. The nonstructured N-terminal is missing in Eg14-3-3.5 and is 6−17 aa long for the other isoforms. The nonstructured C-terminal, in turn, is 8−20 aa long, with the shortest being found in Eg14-3-3.3.

As is typical for 14-3-3 protein family members, the Eg14-3-3 isoforms 1−4 are likely to form homodimers, according to our modeling and sequence analysis. Homodimerization of 14-3-3 proteins relies on helices α1−α4, especially on an Arg residue in the α2 helix and a Glu residue in the α4 helix (Arg19 and Glu92, respectively, in the human 14-3-3ε protein used as

DOI: 10.1021/pr5010136
J. Proteome Res. 2015, 14, 1700−1715

reference; Figure S2), involved in the formation salt bridges between protein monomers.[27,43] The Eg14-3-3.1−4 isoforms all present typical sets of α1−α4 helices and the conserved Arg and Glu residues (Figure S2). Homodimer formation may not occur in Eg14-3-3.5, which misses the α1 helix and the conserved Arg residue in the α2 helix, and in Eg14-3-3.6, in which the conserved α2 helix Arg residue is replaced by a Leu residue.

The 14-3-3 protein dimer structure forms a groove in which two phosphoprotein-binding sites are found, one in each monomer.[43] Typically, a set of five conserved residues (Arg57, Arg130, Tyr131, Asn176, and Asn227 in the human 14-3-3ε protein used as reference; Figure S2) is important for the primary interaction with client phosphorylated proteins.[27] All of these residues were found in the Eg14-3-3.1−6 isoforms. Secondary, additional interactions between 14-3-3 proteins and their protein clients rely on the flexible loop between the α8 and α9 helices. This loop is considered to be of critical importance for the specificity of the interactions between each isoform and its targets in a phosphorylation-independent manner.[27,44] In the Eg14-3-3.1−6 proteins, the loop between the α8 and α9 helices is somewhat variable, which may define differences among isoform ligand repertoires.

Amino and carboxyl unstructured end regions of 14-3-3 proteins, as those found in Eg14-3-3 isoforms, are more divergent than the core protein region and may interact with isoform-specific client proteins and/or confer specialized subcellular and tissue localization.[42] It has been speculated that the C-terminal end functions as a suppressor of unspecific interactions between 14-3-3 and ligands.[45]

Expression Analysis of Eg14-3-3 Isoforms in Hydatid Cyst Components

Previous *E. granulosus* RNA-Seq data (see Table S1) reported that the *Eg14-3-3.1−4* genes are the most highly expressed for this family in all of the analyzed parasite stages, from onchosphere to adult.[15,18] Moreover, previous proteomic studies detected the presence of Eg14-3-3.1−4 proteins in *E. granulosus* PSC, excretory/secretory (ES) products, and metacestode components.[7,9] On the basis of their higher expression levels throughout the parasite's life cycle and on their structural features being more similar to *bona fide* 14-3-3 proteins, the Eg14-3-3.1−4 isoforms were selected for further characterization.

Eg14-3-3.1−4 CDS were cloned and expressed in *E. coli*, and isoform-specific anti-Eg14-3-3 sera were raised in rabbits. The specificity of polyclonal antisera to the corresponding protein isoforms was demonstrated by immunoblot (Figure S4), with no detectable cross reactivity under our assay conditions. These antisera were used in immunoblot experiments to further investigate the Eg14-3-3 expression pattern in the pathogenic larval stage of *E. granulosus* (Figure 2). The expression of all four of the Eg14-3-3 isoforms that were analyzed was observed in PSC and GL samples from the different tested parasite cysts. No Eg14-3-3 isoform was detected in *E. granulosus* HCF.

Our immunoblot results regarding Eg14-3-3 expression agree with previous transcriptional and proteomic studies that reported the expression of Eg14-3-3.1−4 isoforms at the *E. granulosus* pathogenic larval stage. Zheng et al.[15] and Tsai et al.[18] reported *Eg14-3-3.1* and *Eg14-3-3.3* genes as having higher expression levels in parasite metacestode. Although this differential expression is not obvious for PSC samples tested, Eg14-3-3.1 and Eg14-3-3.3 were found here to be over-

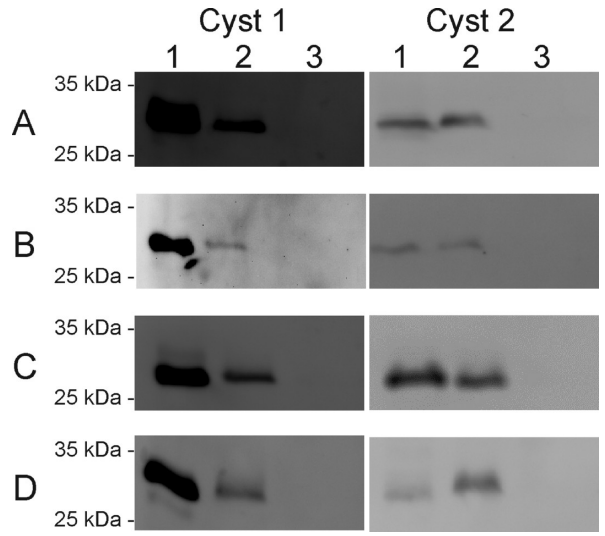

Figure 2. Analysis of the Eg14-3-3 protein expression pattern in *E. granulosus* metacestodes. Proteins from PSCs (1), GL (2), and HCF (3) were analyzed by immunoblot with isoform-specific antisera against (A) Eg14-3-3.1, (B) Eg14-3-3.2, (C) Eg14-3-3.3, and (D) Eg14-3-3.4 in individual *E. granulosus* (1 and 2) cysts.

represented among the Eg14-3-3 isoforms that were expressed in the germinal layer. Although Eg14-3-3.1−4 isoforms have been identified in ES products of *in vitro*-cultured *E. granulosus* PSC,[9] we were not able to detect any of these isoforms in *E. granulosus* HCF samples. Such differences could be explained by the higher sensitivity of proteomic methods and by possible qualitative and quantitative differences between proteins secreted *in vitro* and *in vivo* by PSC. Moreover, differences in Eg14-3-3 isoform expression and secretion may be related to physiological variations in cyst conditions and host response during infection.

We also performed immunofluorescence assays (whole-mount and sections) to determine the Eg14-3-3 spatial expression profile in *E. granulosus* metacestode (Figures 3 and 4). These experiments revealed the presence of the four Eg14-3-3 isoforms that are widely distributed in all cell types of PSC (Figures 3 and S5), which agrees with the reported wide distribution of 14-3-3 proteins in eukaryotic cells.[16] Eg14-3-3 proteins were also detected on the tegument surface of PSC in both whole-mount and section samples. In whole-mount PSC samples, it was possible to observe Eg14-3-3.2 and Eg14-3-3.4 staining in nerve cords and their colocalization with actin (the arrows in Figure 3E). The four Eg14-3-3 isoforms were also detected in the parasite germinal layer (Figure 4), with the Eg14-3-3.4 isoform also found associated with the laminar layer.

The presence of Eg14-3-3 isoforms in components that represent host−parasite interfaces, such as the CW, PSC, and tegument, is suggestive of possible roles for these proteins in host−interaction molecular mechanisms as well as their active presentation to host immune system. The participation of Eg14-3-3 proteins in the evasion of the host cellular immune response during parasite infection by inhibiting nitric oxide production by macrophages has been described.[46] There is also accumulating evidence that 14-3-3 proteins are potential antigens for vaccine and diagnostic tests against hydatid disease.[16] The presence of two Eg14-3-3 isoforms in nerve cords is suggestive of both isoform functional specialization and the involvement of 14-3-3 proteins with neural development in

DOI: 10.1021/pr5010136
J. Proteome Res. 2015, 14, 1700−1715

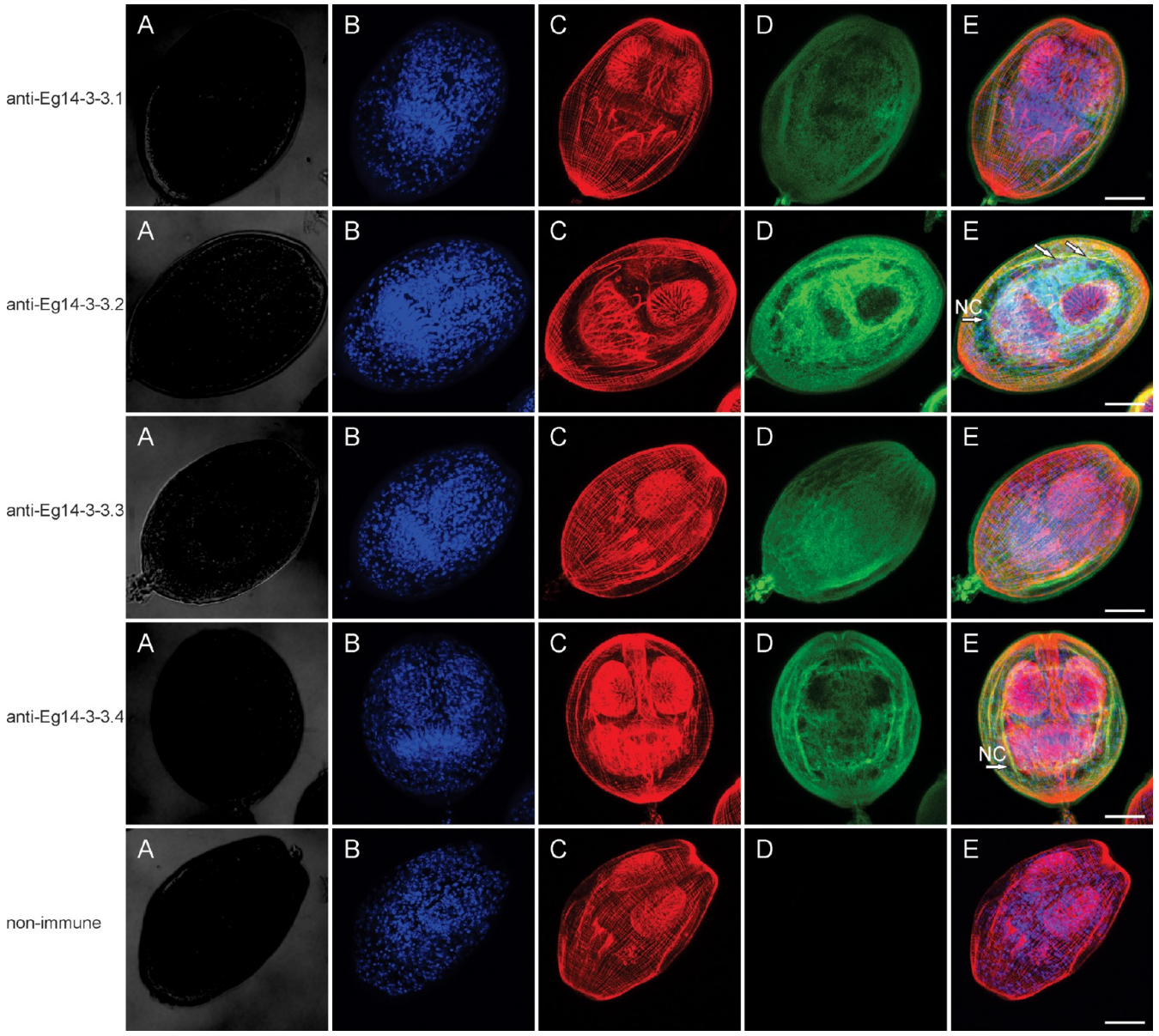

Figure 3. Analysis of the spatial expression pattern of Eg14-3-3 isoforms in *E. granulosus* whole-mount PSC by immunofluorescence: (A) bright field, (B) DAPI nuclei staining, (C) phalloidin staining, (D) antibody staining (purified isoform-specific anti-Eg14-3-3 or nonimmune IgG), and (E) merge. Recognition of immune complexes was achieved using Alexa 488-conjugated anti-rabbit IgG. In the merged images, white arrows indicate colocalization of antibody staining with phalloidin staining; NC represent nerve cords; scale bars: 30 μm.

E. granulosus. The expression of 14-3-3 in the nervous system has been reported in mammals, where these proteins regulate the subcellular localization of target proteins and may play protective roles against neurodegeneration.[47]

Identification of Protein Ligands for Eg14-3-3.1−4 Isoforms

To gain insight into the cellular functions that are regulated by 14-3-3 proteins in *E. granulosus*, we investigated the repertoire of protein ligands of each of the four major Eg14-3-3 isoforms that are expressed during the parasite larval stage (Eg14-3-3.1−4). The recombinant Eg14-3-3.1−4 isoforms were used in three distinct and complementary interaction assays (2D gel overlay, cross-linking and affinity chromatography) to detect or isolate their protein ligands among *E. granulosus* PSC proteins. The Eg14-3-3-binding proteins that were detected or recovered in these assays were subsequently identified by mass spectrometry (Figure 5 and Tables S4−S6).

Control experiments using the GST protein were performed for all of the interaction assays in order to demonstrate the specificity of our experimental approaches. Additional control experiments were performed for 2D gel overlay using Eg14-3-3 recombinant isoforms that were preincubated with the R18 peptide (Figure S6). In this control assay, a signal reduction was observed due to the peptide competition for 14-3-3 binding, which also highlighted the specificity of the protein−protein interactions that were identified by this method.

As shown in Table 1, 2D gel overlay, cross-linking, and affinity chromatography assays using Eg14-3-3 recombinant proteins recovered 27, 58, and 18 nonredundant binding partners from PSC extracts, respectively. Overall, the use of these three different experimental approaches permitted the identification of 95 nonredundant Eg14-3-3-interacting pro-

DOI: 10.1021/pr5010136
J. Proteome Res. 2015, 14, 1700−1715

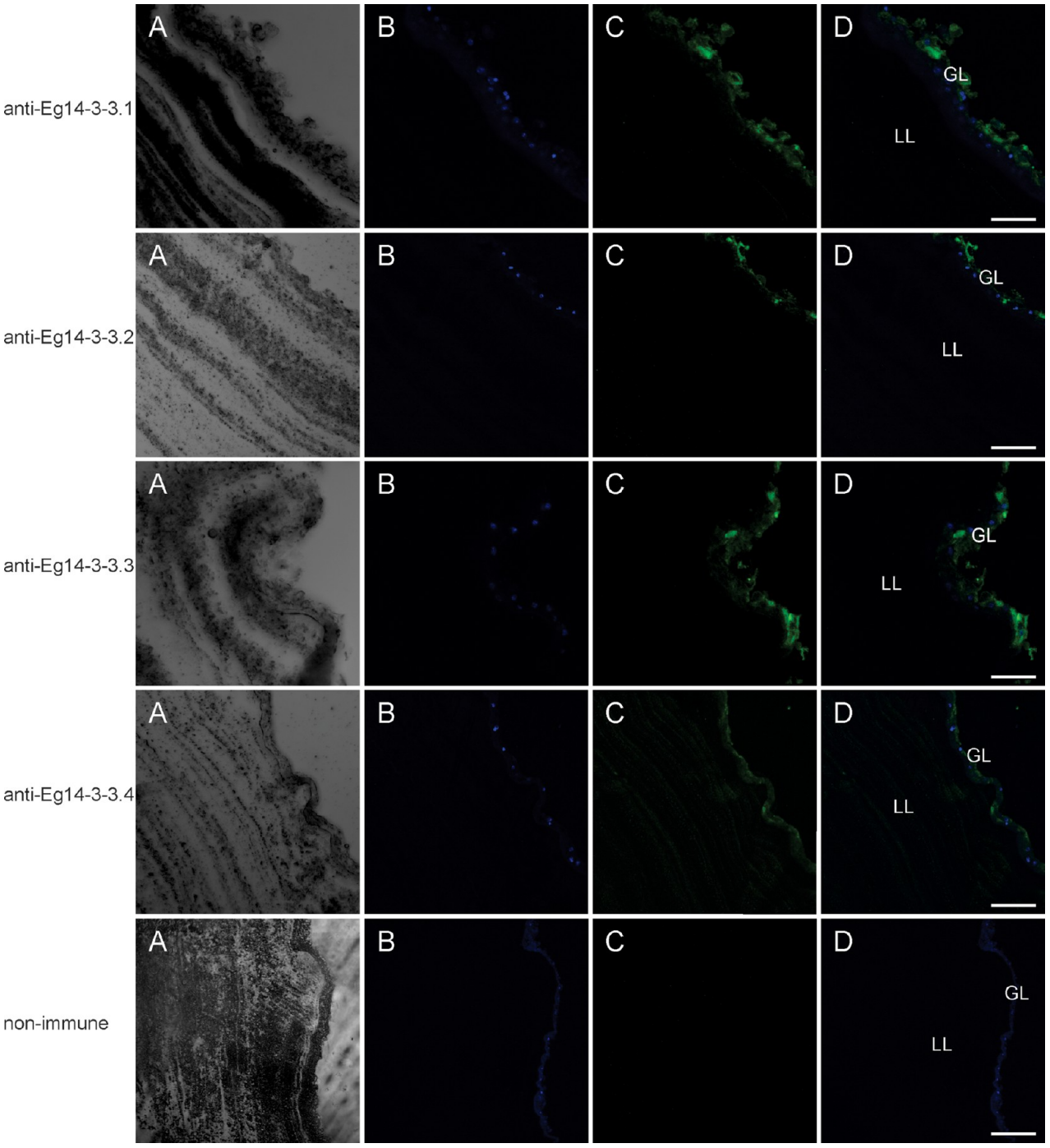

Figure 4. Analysis of Eg14-3-3 expression pattern in *E. granulosus* CW sections (5 μm) by immunofluorescence: (A) bright field, (B) DAPI nuclei staining, (C) antibody staining (purified isoform-specific anti-Eg14-3-3 or nonimmune IgG), and (D) merge. Detection of immune complexes was achieved using Alexa 488-conjugated anti-rabbit secondary antibodies; scale bars: 30 μm.

teins, with little overlapping between the ligand protein sets that were identified by the used methods.

This result is likely due to the distinct types of protein−protein interactions that are targeted by each technique. 2D gel overlay detects only more abundant and soluble proteins[48] and direct protein−protein interactions,[37] thus restricting the number of cellular proteins and interactions that can be assayed by this method. In addition, affinity chromatography using a specific competitor (R18 peptide) is especially useful in identifying *bona fide* Eg14-3-3 targets and indirect protein−protein interactions as well.[37] Cross-linking assays, in turn, permit the identification of transient protein−protein interactions because the use of the Sulfo-SBED reagent covalently stabilizes protein interactions. This stabilization agrees with the higher number of Eg14-3-3-binding proteins that were identified by this experimental approach compared to the other two.

A KOG functional annotation of the whole set of nonredundant Eg14-3-3 ligands (Table 1; data summarized in Figure 6A) revealed that these ligands are related to a wide range of biological functions, with most of them belonging to Z (cytoskeleton 16%), O (post-translational modification, protein

DOI: 10.1021/pr5010136
J. Proteome Res. 2015, 14, 1700−1715

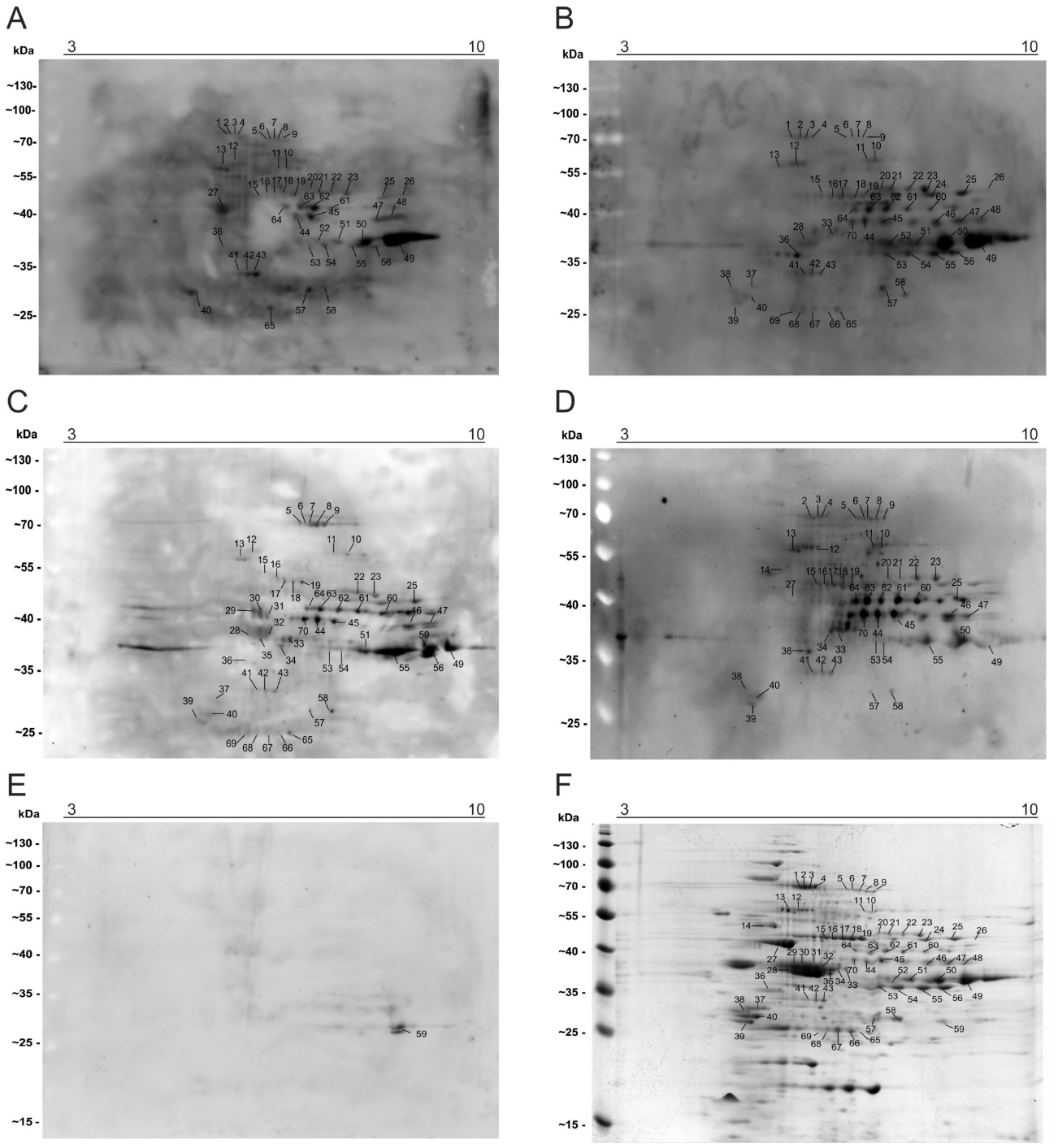

Figure 5. Detection of Eg14-3-3-binding proteins in *E. granulosus* protoscolex extract by two-dimensional gel overlay assay. Protoscolex proteins were separated on a linear pH range of 3−10 in the first dimension and in 12% SDS-PAGE in the second dimension. The membranes were incubated with recombinant proteins (A) Eg14-3-3.1, (B) Eg14-3-3.2, (C) Eg14-3-3.3, (D) Eg14-3-3.4, or (E) GST tagged with biotin. Protein−protein interactions were detected with streptavidin−peroxidase conjugate. (F) 2-DE of *E. granulosus* protoscolex proteins showing the spots corresponding to detected Eg14-3-3-binding proteins. Spots were numbered, and their MS data are shown in Table S5. Molecular weight markers are shown on the left.

turnover, and chaperones 15%), C (energy production and conversion 12%), G (carbohydrate transport and metabolism 9%), J (translation 7%), and U (intracellular trafficking and secretion 6%). Other classes were represented by less than 6% of the identified proteins. Our results indicate that Eg14-3-3.1−4 isoforms are involved in multiple cellular processes in *E. granulosus*. The overall repertoire of Eg14-3-3 target proteins is similar to that reported for 14-3-3 proteins from different organisms,[37,49−51] with the cytoskeleton, metabolism, and chaperones representing the most abundant functional categories.

The Venn diagram in Figure 6B shows that 21% (20 out of 95) of the overall repertoire of the identified Eg14-3-3 ligands is shared by the four isoforms. The other 25% (24 out of 95) is shared with two or three isoforms. These overlaps in ligand repertoires suggest some degree of functional redundancy, as

DOI: 10.1021/pr5010136
J. Proteome Res. 2015, 14, 1700−1715

Table 1. Eg14-3-3 Protein Ligands That Were Identified in PSC Extracts from *E. granulosus*

protein name	protein accession nos.[a]	functional classification[b]	Eg14-3-3 isoform[c]			
			Eg14-3-3.1	Eg14-3-3.2	Eg14-3-3.3	Eg14-3-3.4
Exclusive Eg14-3-3.1-Binding Proteins						
heat shock protein 70	EgrG_001065400	O	*c*			
sco cytochrome oxidase deficient protein 1	EgrG_000228900	C	*c*			
dynein light chain	EgrG_000940500	Z	*c*			
inosine 5′ monophosphate dehydrogenase 2	EgrG_000120200	F	*c*			
ras protein Rab 27A	EgrG_000347300	U	*c*			
rho gdp dissociation inhibitor	EgrG_001152900	T	*c*			
ribosomal protein L11	EgrG_000177700	J	*c*			
Exclusive Eg14-3-3.2-Binding Proteins						
glycerol 3 phosphate dehydrogenase	EgrG_000964600	C		*c*		
succinyl coenzyme A synthetase alpha subunit	EgrG_001199000	C		*c*		
synaptic vesicle membrane protein VAT 1	EgrG_000935200	C		*a*		
actin protein 2B	EgrG_000801400	Z		*c*		
actin protein 3B	EgrG_000292600	Z		*c*		
profilin	EgrG_000122100	Z		*c*		
tubulin beta 2C chain	EgrG_000672200	Z		*a*		
hypoxanthine guanine phosphoribosyltransferase	EgrG_000758800	F		*c*		
dehydrogenase:reductase SDR family	EgrG_000410100	Q		*c*		
transmembrane emp24 domain containing protein	EgrG_000574700	U		*c*		
threonyl tRNA synthetase C	EgrG_000375800	J		*c*		
protease inhibitor serine	EgrG_001193100	V		*c*		
atlastin 2	EgrG_000707700	R		*a*		
ras protein Rap 1b	EgrG_000859400	R		*c*		
programmed cell death 6 interacting protein	EgrG_000997530	R		*c*		
Exclusive Eg14-3-3.3-Binding Proteins						
dolichyl diphosphooligosaccharide protein	EgrG_000996800	O			*c*	
heat shock 10 kDa protein 1	EgrG_000320800	O			*c*	
heat shock protein 90 alpha	EgrG_000008700	O			*a*	
acetyl coenzyme A hydrolase transferase	EgrG_001087900	C			*c*	
aldehyde dehydrogenase mitochondrial	EgrG_000389100	C			*c*	
lactate dehydrogenase a	EgrG_000660800	C			*c*	
NADP dependent malic enzyme	EgrG_000645800	C			*c*	
dynein heavy chain	EgrG_000832000	Z			*c*	
fascin 2	EgrG_000181100	Z			*c*	
GTP binding protein SAR1b	EgrG_000100200	U			*c*	
ras protein Rab 2A	EgrG_000430800	U			*c*	
abnormal embryogenesis family member emb 9	EgrG_000144400	W			*a*	
collagen alpha 1 V chain	EgrG_000144300	W			*a*	
G1Y162 protein	EgrG_000515900	W			*c*	
integrin beta 2	EgrG_000528400	W			*c*	
basement membrane specific heparan sulfate	EgrG_000701800	T			*a*	
40s ribosomal protein S16	EgrG_000821300	J			*c*	
arginyl tRNA synthetase cytoplasmic	EgrG_000348100	J			*c*	
elongation factor 1 alpha	EgrG_000982200	J			*a*	
PUR alpha protein	EgrG_000780600	K			*c*	
zinc finger protein 26	EgrG_000920300	K			*c*	
pre mRNA processing factor 39	EgrG_000379000	A			*c*	
expressed conserved protein	EgrG_000470500	S			*c*	
tetraspanin	EgrG_000355700	S			*c*	
protein memo1	EgrG_000237250	R			*c*	
major vault protein	EgrG_000142500	No KOG			*a*	
Exclusive Eg14-3-3.4-Binding Proteins						
carbonyl reductase 1	EgrG_000115200	Q				*c*
seryl tRNA synthetase	EgrG_001197300	J				*t*
splicing factor 3b subunit 3	EgrG_000633300	A				*c*
Complete Sharing by Four Eg14-3-3 Isoforms						
6 phosphofructokinase	EgrG_001128600	G	*c*	*c*	*c*	*c*
enolase	EgrG_000514200	G	*t*	*t*	*t*	*t*
fructose 1,6 bisphosphate aldolase	EgrG_000905600	G	*t*	*t*	*t*	*t*

DOI: 10.1021/pr5010136
J. Proteome Res. 2015, 14, 1700−1715

Table 1. continued

protein name	protein accession nos.[a]	functional classification[b]	Eg14-3-3 isoform[c]			
			Eg14-3-3.1	Eg14-3-3.2	Eg14-3-3.3	Eg14-3-3.4
Complete Sharing by Four Eg14-3-3 Isoforms						
glucose 6 phosphate isomerase	EgrG_000626300	G	*t*	*t*	*t*	*t*
glyceraldehyde 3 phosphate dehydrogenase	EgrG_000254600	G	*t*	*t*	*t*	*t*
phosphoglycerate mutase	EgrG_000799500	G	*t*	*t*	*t/c*	*t*
heat shock 70 kDa protein 4	EgrG_001085400	O	*t*	*t*	*a*	*t/a*
Eg14-3-3.1	EgrG_001192500	O	*t/a*	*t*	*t*	*t*
protein disulfide isomerase A3	EgrG_001022300	O	*t*	*t*	*t*	*t*
citrate synthase	EgrG_001028500	C	*t*	*t*	*t*	*t*
cytosolic malate dehydrogenase	EgrG_000417100	C	*t*	*t*	*t*	*t*
phosphoenolpyruvate carboxykinase	EgrG_000292700	C	*t*	*t*	*t/a*	*t*
F actin capping protein subunit beta	EgrG_000772300	Z	*c*	*c*	*c*	*c*
gelsolin	EgrG_000882300	Z	*t*	*t*	*t*	*t*
methylthioadenosine phosphorylase	EgrG_000622900	F	*t*	*t*	*t*	*t*
aspartate aminotransferase mitochondrial	EgrG_001134100	E	*t*	*t*	*t*	*t*
UDP glucose 4 epimerase	EgrG_000984800	M	*t*	*t*	*t*	*t*
annexin	EgrG_000244000	U	*t*	*t*	*t*	*t*
cAMP dependent protein kinase regulatory	EgrG_000775600	T	*t*	*t*	*t*	*t*
major egg antigen p40	EgrG_000212700	No KOG	*t*	*t*	*t/a*	*t*
Partial Sharing by Two or Three Eg14-3-3 Isoforms						
alpha N acetylgalactosaminidase	EgrG_000340500	G	*c*	*c*		
phosphoglycerate kinase 1	EgrG_001043100	G	*t*	*t*		*t*
UTP glucose 1 phosphate uridylyltransferase	EgrG_000843500	G		*c*	*c*	
Eg14-3-3.2	EgrG_000231300	O		*t/a*	*t*	
Eg14-3-3.3	EgrG_000364000	O		*t*	*t/a*	*t*
Eg14-3-3.4	EgrG_001060100	O		*t*		*t/c/a*
heat shock protein 60	EgrG_001190900	O	*c*	*c*	*c*	
ubiquitin carboxyl terminal hydrolase 7	EgrG_000875300	O			*c*	*c*
ubiquitin modifier activating enzyme 1	EgrG_000711500	O		*c*	*c*	
polyubiquitin	EgrG_000516500	O			*c*	*c*
actin	EgrG_000061200	Z	*t*			*t*
actin cytoplasmic type 5	EgrG_000190400	Z			*a*	*a*
fimbrin	EgrG_000786800	Z	*c*		*c*	
filamin	EgrG_000859700	Z			*c*	*c*
kinesin heavy chain	EgrG_001025000	Z	*c*			*c*
tubulin alpha chain	EgrG_000886400	Z	*c*	*c*	*c*	
3 oxoacyl acyl carrier protein reductase	EgrG_000792800	Q	*c*		*c*	
glutamine: fructose 6 phosphate aminotransferase	EgrG_000097800	M		*c*	*c*	
annexin	EgrG_000193700	U		*t*	*t*	*t*
collagen alpha 1(IV) chain	EgrG_000144350	W		*a*	*a*	*a*
endophilin B1	EgrG_000550800	T		*t*	*t*	
expressed conserved protein	EgrG_000213800	J	*c*	*c*		
dipeptidyl peptidase 3	EgrG_001028100	R		*c*	*c*	
ETHE1 protein	EgrG_001090400	R	*t*	*t*	*t*	

[a]Protein accession numbers according to GeneDB (www.genedb.org). [b]Functional classification was determined using eukaryotic orthologous group (KOG). [c]Eg14-3-3 isoform(s) to which the protein binds. The method(s) that was used to demonstrate binding is indicated as follows: (*t*) two-dimensional gel overlay, (*c*) cross-linking assays, and (*a*) affinity chromatography.

previously shown in other organisms with 14-3-3 isoforms with overlapping ligand profiles.[52] Thus, some functions could be carried out by more than one 14-3-3 isoform.

In addition, 54% (51 out of 95) of the Eg14-3-3-binding proteins were exclusive from a single isoform under our experimental conditions, suggesting a certain degree of functional specialization. Previous studies with other eukaryotic organisms strongly suggest that there is indeed functional specialization for 14-3-3 isoforms that is associated with their differential expression and ability to bind different ligands.[52,53] Therefore, it is likely that *E. granulosus* 14-3-3 isoforms have some overlapping functions, whereas other functions may be exclusively performed by a given isoform.

The Eg14-3-3.2 and Eg14-3-3.3 isoforms showed the highest numbers of exclusive binding partners among the identified proteins, with 15 and 26 exclusive ligands, respectively. Regarding Eg14-3-3.3, it presents a shorter C-terminal unstructured end (Figure 1 and S2), which may be associated with a less restrictive structure for ligand binding. Therefore, this could explain, at least in part, the larger repertoire of ligands identified for this protein in comparison to that of the other Eg14-3-3 isoforms.

DOI: 10.1021/pr5010136
J. Proteome Res. 2015, 14, 1700−1715

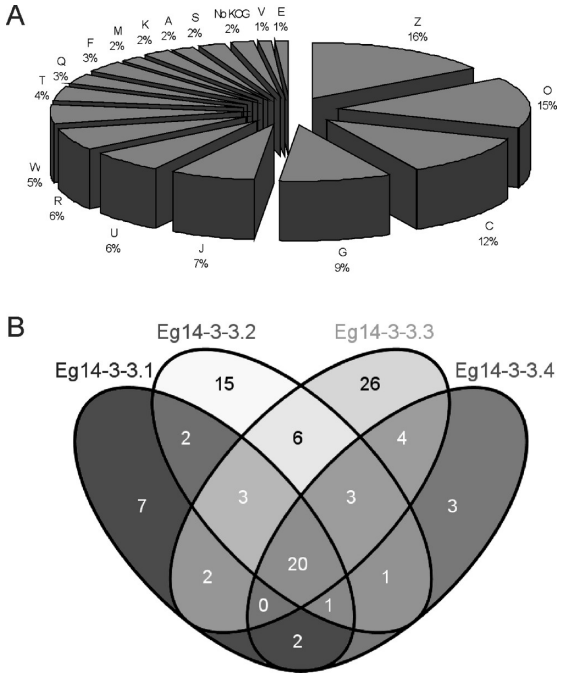

Figure 6. Functional and comparative analysis of Eg14-3-3-binding proteins. (A) Distribution of KOG functional categories of total identified Eg14-3-3-binding proteins. Percentages of proteins identified in each functional category are indicated in the sectors of circle. (Z) Cytoskeleton; (O) post-translational modification, protein turnover, chaperones; (C) energy production and conversion, (G) carbohydrate transport and metabolism; (J) translation; (U) intracellular trafficking and secretion; (R) general function prediction; (W) extracellular structures; (T) signal transduction; (Q) secondary metabolites biosynthesis, transport, and catabolism; (F) nucleotide metabolism and transport; (M) cell wall/membrane/envelope biogenesis; (K) transcription; (A) RNA processing and modification; (V) defense mechanisms; (E) amino acid metabolism and transport; (S) function unknown; and (No KOG) proteins were no KOG related. (B) Venn diagram showing the distribution of protein ligands of each Eg14-3-3 isoform.

For further analysis, the KOG terms that were assigned to Eg14-3-3 ligands were arbitrarily divided into two groups: one of more general functions, as represented by basic metabolism, transport, and structural functions, and another of more specialized functions, including transcription, RNA processing and modification, signal transduction, and other functions (Figure 7). The repertoire of binding proteins that is shared by four, three, or two Eg14-3-3 isoforms is mostly represented by proteins that are involved in general functions (Figure 7A), such as carbohydrate transport and metabolism (G), cytoskeleton (Z), and post-translational modification, protein turnover, and chaperones (O). In addition, a higher number of Eg14-3-3-binding proteins that are involved in more specialized functions were found in the set of proteins that exclusively interact with a single Eg14-3-3 isoform compared to that of the repertoire of ligands that are shared by the Eg14-3-3 isoforms (Figure 7B–E). These isoform-specific ligands are related to functions such as transcription (K), extracellular structures (W), unknown function (S), translation (J), and intracellular trafficking and secretion (U).

Among the set of functions, proteins that interact exclusively with the Eg14-3-3.3 isoform (Figure 7D) represent the largest number of functional categories (9 KOG terms) compared to the repertoires of exclusive ligands from the other assessed

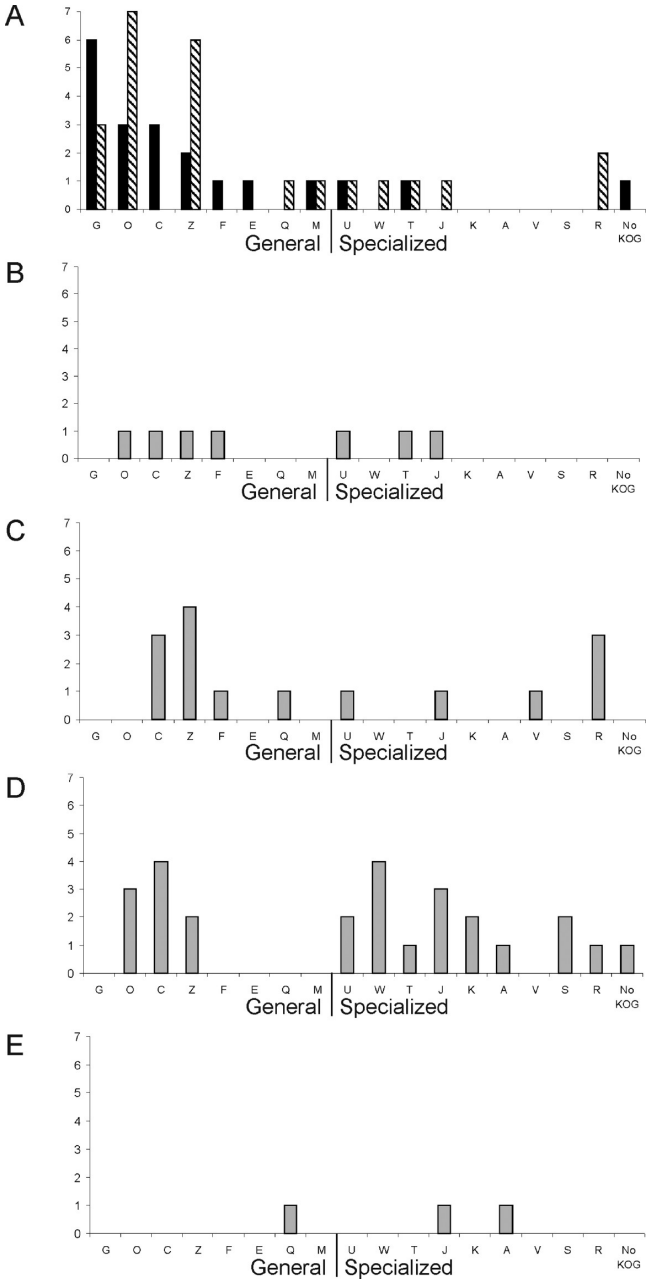

Figure 7. Functional distribution of Eg14-3-3-binding proteins shared or exclusive for each isoform according to KOG functional categories. (A) Eg14-3-3-binding proteins shared by all isoforms (black bars) and by two or three isoforms (cross-hatched bars). Proteins bound exclusively by the (B) Eg14-3-3.1, (C) Eg14-3-3.2, (D) Eg14-3-3.3, or (E) Eg14-3-3.4 isoform.

Eg14-3-3 isoforms (Figures 7B,C,E). This result suggests the participation of this protein isoform in the regulation of molecular processes as diverse as transcription and intracellular trafficking and secretion, indicating a higher degree of multifunctionality.

Eg14-3-3 proteins were found among the protein ligands that were recovered in our interaction assays, which is in line with the well-documented dimerization of 14-3-3 proteins.[54] Through distinct approaches, we observed that Eg14-3-3.1–4 isoforms are able to form both homo- and heterodimers. Relative protein quantification by spectral counting (Tables S5

DOI: 10.1021/pr5010136
J. Proteome Res. 2015, 14, 1700–1715

and S6) suggested a preference for the homodimeric protein configuration.

Our results indicate that Eg14-3-3 proteins are involved in the regulation of *E. granulosus* central metabolic pathways. In different species, numerous proteins that participate in essential metabolic pathways have been identified as 14-3-3 binding partners.[55] We found several enzymes that are involved in glycolysis among Eg14-3-3 ligands, including phosphofructokinase, phosphoglycerate mutase, enolase, phosphoglycerate kinase, fructose-1,6-bisphosphate aldolase, and glyceraldehyde-3-phosphate dehydrogenase. Glycolysis is a very important pathway for parasite metabolism, as glucose is the main source of fuel for tissues and is also the major respiratory substrate.[56] In addition, interactions between Eg14-3-3 proteins and glycolytic enzymes may have additional functions, as many of them exhibit various nonglycolytic activities known as moonlighting. In *E. granulosus*, fructose-bisphosphate aldolase and enolase are described as moonlighting proteins, and these enzymes are found in host-interacting parasite components.[34]

We also observed that Eg14-3-3 proteins interact with several stress-related proteins, such as heat shock proteins (HSPs). There is evidence supporting the cooperation between these two families of proteins for eukaryotic cell survival to stress. In humans, these interactions increase HSP chaperone activity.[57] In *E. granulosus*, the transcription levels of the genes encoding HSP70, HSP60, and 14-3-3 proteins increased after the treatment of protoscoleces with an antihelminthic.[58] In helminth parasites, such as *E. granulosus*, which survive in hostile environments that are subjected to various stress situations as promoted by the host defense system, the development of strategies for robust defense is critical. Thus, the interaction between HSPs and 14-3-3 protein families is likely of great importance for *E. granulosus* survival under stressful conditions.

Another group of Eg14-3-3-binding proteins that is well-represented in this study is cytoskeletal proteins, which include actin, tubulin, filamin, F-actin capping, dynein, fimbrin, kinesin, and actin filament-fragmenting protein. Eg14-3-3 and actin colocated in immunofluorescence experiments with whole-mount PSC (the white arrows in Figure 3), which corroborate our interaction data. The role of 14-3-3 proteins in the maintenance of cell shape has been described, with an abnormal morphology in mammalian cells after blocking the binding of 14-3-3 proteins to their targets.[59] *E. granulosus* actin filament-fragmenting protein (EgAFFP) is involved in the dynamic rearrangements of the cytoskeleton.[60] Overall, our results suggest that Eg14-3-3 proteins could regulate cytoskeleton dynamic rearrangements, which are required for several *E. granulosus* key cellular and developmental processes, such as motility, cytokinesis, and cytoplasmic organization.[61]

Several proteins that are involved in transcription, RNA processing, and translation were found as partners of Eg14-3-3 isoforms. In previous studies, 14-3-3 proteins have been functionally implicated in signal transduction cascades and gene expression.[10,11,13,62] The suggested involvement of Eg14-3-3 in the regulation of transcription, RNA processing, and translation deserves future investigation to elucidate the role of these proteins in *E. granulosus* survival, development, and adaptability.

Our results also suggest Eg14-3-3 participation in membrane protein delivery to the cell surface, as proteins that are involved in intracellular trafficking were found among Eg14-3-3-binding partners. Proteins that are targeted to membrane/extracellular exposure by Eg14-3-3 could represent important players in host−parasite cross talk, mediating processes such as cell signaling or even immunomodulation. The modulation of the cell-surface targeting of key membrane proteins by 14-3-3 proteins is a physiologically important regulatory mechanism.[63]

The G1Y162 protein and tetraspanin could represent potential targets for membrane/extracellular exposure by the Eg14-3-3.3 isoform. Once in the membrane/extracellular space, these proteins may contribute to immunoregulatory events at the host−parasite interface during infection and represent valuable vaccine and drug target candidates.[56,64,65] This contribution is especially interesting for the G1Y162 protein, as this protein is only similar to proteins from parasites such as *Echinococcus* spp. and *Taenia* spp. Moreover, tetraspanins are protein markers of extracellular vesicles, such as exosomes. Because extracellular vesicles are emerging as novel mechanisms of intercellular communication, being involved in antigen presentation, immunity, and pathogen transmission,[66] it is interesting to speculate a possible role for the Eg14-3-3.3-tetraspanin interaction in this context.

Although Eg14-3-3.1−4 have all been previously detected among PSC ES products,[9] proteins from extracellular structures were mainly found among Eg14-3-3.3 isoform-binding targets. Since eukaryotic 14-3-3 proteins are involved in the regulation of cell−matrix interactions, motility, and migration,[67] our results suggest that the Eg14-3-3.3 isoform could participate in matrix-mediated cell adhesion and signaling events at the *E. granulosus* host−parasite interface. The standardized methods for the assessment of *Echinococcus* protein−protein interactions also paved the way for the investigation of interactions between Eg14-3-3 and host proteins found in the HCF.

CONCLUDING REMARKS

Despite the enormous advances that have been made in the field of 14-3-3 biochemistry, additional studies are necessary to understand the biological implications of 14-3-3 protein interactions. Global studies, such as ours, are useful for a better understanding of the 14-3-3 interactome. Moreover, the study of a parasitic organism allowed us to investigate the 14-3-3-specific interactions that may be relevant for parasite biology, including host−parasite interactions. Eg14-3-3.1−4 isoforms expression patterns were established for *E. granulosus* metacestode components, including those that interact directly with the host (CW and PSC tegument), suggesting possible roles for these proteins in the molecular mechanisms of host−parasite cross-talk, such as immunomodulation. A set of 95 Eg14-3-3 protein ligands was identified with a wide range of biological functions, indicating that Eg14-3-3 proteins are involved in multiple molecular pathways in *E. granulosus*. Among the Eg14-3-3-binding partners, some were previously described for 14-3-3 proteins of other organisms, but new 14-3-3 protein interactions were also reported that could represent parasite-specific protein interactions. Our results revealed that Eg14-3-3 isoforms have shared partners, indicating some overlapping functions, but that they also bind exclusive proteins, suggesting specialized functions. Moreover, the protein ligands that are shared by Eg14-3-3 isoforms were mostly involved in general functions, whereas isoform-specific binding partners were additionally implicated in more specialized functions, such as RNA processing and intracellular trafficking and secretion. In this scenario, the Eg14-3-3.3 isoform is noteworthy, with its binding partners representing the widest range of functional categories. The characterization

DOI: 10.1021/pr5010136
J. Proteome Res. 2015, 14, 1700−1715

of the Eg14-3-3 expression pattern and ligand set indicate important roles for these proteins and their relevance for parasite development and host interactions.

■ ASSOCIATED CONTENT

Supporting Information

Table S1. Structure and transcription profiles of *E. granulosus* 14-3-3 genes and characteristics of the predicted proteins. Table S2. Identity/similarity levels (%) between Eg14-3-3 proteins and 14-3-3 proteins from selected organisms. Table S3. Quality data models of Eg14-3-3 structural modeling. Table S4. Protoscolex proteins that were identified by 2-DE/MALDI-Q-TOF MS/MS. Table S5. MS data from Sulfo-SBED cross-linking assays. Table S6. MS data from Eg14-3-3-affinity chromatography. Figure S1. Diagrammatic representation of the exon-intron structures of *E. granulosus* 14-3-3 genes (*Eg14-3-3.1*−*6*). Figure S2. Multiple alignment of the Eg14-3-3 amino acid sequences. Figure S3. Phylogenetic analysis of the Eg14-3-3 proteins. Figure S4. Specificity analysis of anti-Eg14-3-3 antibodies by immunoblot using recombinant proteins. Figure S5. Analysis of the spatial expression pattern of Eg14-3-3 isoforms by immunofluorescence in *E. granulosus* protoscolex sections. Figure S6. Analysis of the R18 peptide effect in Eg14-3-3 recombinant binding to protoscolex proteins by one-dimensional gel overlay.Figure S6. One-dimensional gel overlay analysis of the R18 peptide effect on Eg14-3-3 recombinant binding to protoscolex proteins. This material is available free of charge via the Internet at http://pubs.acs.org.

■ AUTHOR INFORMATION

Corresponding Author

*Tel.: +55 51 3308 7768; Fax: +55 51 3308 7309; E-mail: henrique@cbiot.ufrgs.br.

Author Contributions

‖A.T. and D.M.V. contributed equally to this work.

Notes

The authors declare no competing financial interest.

■ ACKNOWLEDGMENTS

We thank Dr. Magdalena Zarowiecki (Parasite Genomics Group, Wellcome Trust Sanger Institute) for *Echinococcus* genomic and transcriptomic data, Dr. Sarah Meek for helpful discussions about the 14-3-3 gel overlay experiments, and Dr. Claudia Elizabeth Thompson for help with phylogenetic analyses and 3D modeling. We also thank the Brazilian Biosciences National Laboratory (LNBio, Campinas, Brazil) (under proposal nos. MAS-13423 and MAS-16458) and Uniprote-MS (Cbiot/UFRGS) for LC−MS/MS analyses and the Centro de Microscopia Eletrônica (UFRGS) for technical support with confocal microscopy. This work was supported by CAPES (AUX-PE-PARASITOLOGIA-1278/2011) and CNPq (Proj. 490923/2008-9) in Brazil and by CONICYT and FONDECYT (1130113 and 1130717) in Chile. A.T. was a recipient of a CAPES Ph.D. fellowship, D.M.V. was a recipient of a CAPES M.Sc. fellowship, K.M.M. was a recipient of a PRODOC/CAPES postdoctoral fellowship, B.V.M. was a recipient of a FAPERGS graduate fellowship, and C.S.D. was a recipient of a FAPERGS graduate fellowship.

■ REFERENCES

(1) Nakao, M.; Lavikainen, A.; Yanagida, T.; Ito, A. Phylogenetic systematics of the genus *Echinococcus* (Cestoda: Taeniidae). *Int. J. Parasitol.* **2013**, *43*, 1017−29.

(2) Balbinotti, H.; Santos, G. B.; Badaraco, J.; Arend, A. C.; Graichen, D.; Haag, K. L.; Zaha, A. *Echinococcus ortleppi* (G5) and *Echinococcus granulosus* sensu stricto (G1) loads in cattle from Southern Brazil. *Vet Parasitol.* **2012**, *188*, 255−60.

(3) Alvarez Rojas, C. A.; Romig, T.; Lightowlers, M. W. *Echinococcus granulosus* sensu lato genotypes infecting humans—review of current knowledge. *Int. J. Parasitol.* **2014**, *44*, 9−18.

(4) de la Rue, M. L.; Takano, K.; Brochado, J. F.; Costa, C. V.; Soares, A. G.; Yamano, K.; Yagi, K.; Katoh, Y.; Takahashi, K. Infection of humans and animals with *Echinococcus granulosus* (G1 and G3 strains) and *E. ortleppi* in Southern Brazil. *Vet Parasitol.* **2011**, *177*, 97−103.

(5) Díaz, A.; Casaravilla, C.; Irigoín, F.; Lin, G.; Previato, J. O.; Ferreira, F. Understanding the laminated layer of larval *Echinococcus* I: structure. *Trends Parasitol.* **2011**, *27*, 204−13.

(6) Siracusano, A.; Riganò, R.; Ortona, E.; Profumo, E.; Margutti, P.; Buttari, B.; Delunardo, F.; Teggi, A. Immunomodulatory mechanisms during *Echinococcus granulosus* infection. *Exp. Parasitol.* **2008**, *119*, 483−9.

(7) Monteiro, K.; de Carvalho, M.; Zaha, A.; Ferreira, H. Proteomic analysis of the *Echinococcus granulosus* metacestode during infection of its intermediate host. *Proteomics* **2010**, *10*, 1985−1999.

(8) Aziz, A.; Zhang, W.; Li, J.; Loukas, A.; McManus, D. P.; Mulvenna, J. Proteomic characterisation of *Echinococcus granulosus* hydatid cyst fluid from sheep, cattle and humans. *J. Proteomics* **2011**, *74*, 1560−72.

(9) Virginio, V. G.; Monteiro, K. M.; Drumond, F.; de Carvalho, M. O.; Vargas, D. M.; Zaha, A.; Ferreira, H. B. Excretory/secretory products from *in vitro*-cultured *Echinococcus granulosus* protoscoleces. *Mol. Biochem. Parasitol.* **2012**, *183*, 15−22.

(10) Pozuelo Rubio, M.; Geraghty, K. M.; Wong, B. H.; Wood, N. T.; Campbell, D. G.; Morrice, N.; Mackintosh, C. 14-3-3-affinity purification of over 200 human phosphoproteins reveals new links to regulation of cellular metabolism, proliferation and trafficking. *Biochem. J.* **2004**, *379*, 395−408.

(11) Kjarland, E.; Keen, T. J.; Kleppe, R. Does isoform diversity explain functional differences in the 14-3-3 protein family? *Curr. Pharm. Biotechnol.* **2006**, *7*, 217−23.

(12) Lalle, M.; Camerini, S.; Cecchetti, S.; Sayadi, A.; Crescenzi, M.; Pozio, E. Interaction network of the 14-3-3 protein in the ancient protozoan parasite *Giardia duodenalis*. *J. Proteome Res.* **2012**, *11*, 2666−83.

(13) Bridges, D.; Moorhead, G. 14-3-3 proteins: a number of functions for a numbered protein. *Sci. STKE* **2005**, *2005*, re10.

(14) Victor, B.; Kanobana, K.; Gabriël, S.; Polman, K.; Deckers, N.; Dorny, P.; Deelder, A. M.; Palmblad, M. Proteomic analysis of *Taenia solium* metacestode excretion−secretion proteins. *Proteomics* **2012**, *12*, 1860−9.

(15) Zheng, H.; Zhang, W.; Zhang, L.; Zhang, Z.; Li, J.; Lu, G.; Zhu, Y.; Wang, Y.; Huang, Y.; Liu, J.; Kang, H.; Chen, J.; Wang, L.; Chen, A.; Yu, S.; Gao, Z.; Jin, L.; Gu, W.; Wang, Z.; Zhao, L.; Shi, B.; Wen, H.; Lin, R.; Jones, M. K.; Brejova, B.; Vinar, T.; Zhao, G.; McManus, D. P.; Chen, Z.; Zhou, Y.; Wang, S. The genome of the hydatid tapeworm *Echinococcus granulosus*. *Nat. Genet.* **2013**, *45*, 1168−75.

(16) Siles-Lucas, M.; Merli, M.; Gottstein, B. 14-3-3 proteins in *Echinococcus*: their role and potential as protective antigens. *Exp. Parasitol.* **2008**, *119*, 516−23.

(17) Salazar-Anton, F.; Lindh, J. *Taenia solium*: a two-dimensional western blotting method combined with the use of an EST-library for the identification of immunogenic proteins recognized by sera from neurocysticercosis patients. *Exp. Parasitol.* **2011**, *128*, 371−6.

(18) Tsai, I. J.; Zarowiecki, M.; Holroyd, N.; Garciarrubio, A.; Sanchez-Flores, A.; Brooks, K. L.; Tracey, A.; Bobes, R. J.; Fragoso, G.; Sciutto, E.; Aslett, M.; Beasley, H.; Bennett, H. M.; Cai, J.; Camicia, F.; Clark, R.; Cucher, M.; De Silva, N.; Day, T. A.; Deplazes, P.; Estrada,

DOI: 10.1021/pr5010136
J. Proteome Res. 2015, 14, 1700−1715

K.; Fernández, C.; Holland, P. W.; Hou, J.; Hu, S.; Huckvale, T.; Hung, S. S.; Kamenetzky, L.; Keane, J. A.; Kiss, F.; Koziol, U.; Lambert, O.; Liu, K.; Luo, X.; Luo, Y.; Macchiaroli, N.; Nichol, S.; Paps, J.; Parkinson, J.; Pouchkina-Stantcheva, N.; Riddiford, N.; Rosenzvit, M.; Salinas, G.; Wasmuth, J. D.; Zamanian, M.; Zheng, Y.; *Taenia solium* Genome Consortium; Cai, X.; Soberón, X.; Olson, P. D.; Laclette, J. P.; Brehm, K.; Berriman, M. The genomes of four tapeworm species reveal adaptations to parasitism. *Nature* **2013**, *496*, 57−63.

(19) Fernández, C.; Gregory, W.; Loke, P.; Maizels, R. Full-length-enriched cDNA libraries from *Echinococcus granulosus* contain separate populations of oligo-capped and trans-spliced transcripts and a high level of predicted signal peptide sequences. *Mol. Biochem. Parasitol.* **2002**, *122*, 171−80.

(20) Siles-Lucas, M.; Nunes, C.; Zaha, A.; Breijo, M. The 14-3-3 protein is secreted by the adult worm of *Echinococcus granulosus*. *Parasite Immunol.* **2000**, *22*, 521−8.

(21) Besemer, J.; Borodovsky, M. GeneMark: web software for gene finding in prokaryotes, eukaryotes and viruses. *Nucleic Acids Res.* **2005**, *33*, W451−4.

(22) Salamov, A. A.; Solovyev, V. V. Ab initio gene finding in *Drosophila* genomic DNA. *Genome Res.* **2000**, *10*, 516−22.

(23) Burge, C. B.; Karlin, S. Finding the genes in genomic DNA. *Curr. Opin. Struct. Biol.* **1998**, *8*, 346−54.

(24) Saitou, N.; Nei, M. The neighbor-joining method: a new method for reconstructing phylogenetic trees. *Mol. Biol. Evol.* **1987**, *4*, 406−25.

(25) Tamura, K.; Stecher, G.; Peterson, D.; Filipski, A.; Kumar, S. MEGA6: Molecular Evolutionary Genetics Analysis version 6.0. *Mol. Biol. Evol.* **2013**, *30*, 2725−9.

(26) da Fonsêca, M. M.; Zaha, A.; Caffarena, E. R.; Vasconcelos, A. T. Structure-based functional inference of hypothetical proteins from *Mycoplasma hyopneumoniae*. *J. Mol. Model.* **2012**, *18*, 1917−25.

(27) Yang, X.; Lee, W.; Sobott, F.; Papagrigoriou, E.; Robinson, C.; Grossmann, J.; Sundström, M.; Doyle, D.; Elkins, J. Structural basis for protein-protein interactions in the 14-3-3 protein family. *Proc. Natl. Acad. Sci. U.S.A.* **2006**, *103*, 17237−42.

(28) Würtele, M.; Jelich-Ottmann, C.; Wittinghofer, A.; Oecking, C. Structural view of a fungal toxin acting on a 14-3-3 regulatory complex. *EMBO J.* **2003**, *22*, 987−94.

(29) Takala, H.; Nurminen, E.; Nurmi, S. M.; Aatonen, M.; Strandin, T.; Takatalo, M.; Kiema, T.; Gahmberg, C. G.; Ylänne, J.; Fagerholm, S. C. Beta2 integrin phosphorylation on Thr758 acts as a molecular switch to regulate 14-3-3 and filamin binding. *Blood* **2008**, *112*, 1853−62.

(30) Liu, D.; Bienkowska, J.; Petosa, C.; Collier, R. J.; Fu, H.; Liddington, R. Crystal structure of the zeta isoform of the 14-3-3 protein. *Nature* **1995**, *376*, 191−4.

(31) Molzan, M.; Weyand, M.; Rose, R.; Ottmann, C. Structural insights of the MLF1/14-3-3 interaction. *FEBS J.* **2012**, *279*, 563−71.

(32) Brokx, S. J.; Wernimont, A. K.; Dong, A.; Wasney, G. A.; Lin, Y. H.; Lew, J.; Vedadi, M.; Lee, W. H.; Hui, R. Characterization of 14-3-3 proteins from *Cryptosporidium parvum*. *PLoS One* **2011**, *6*, e14827.

(33) Eswar, N.; Webb, B.; Marti-Renom, M. A.; Madhusudhan, M. S.; Eramian, D.; Shen, M. Y.; Pieper, U.; Sali, A. Comparative protein structure modeling using MODELLER. *Current Protocols in Protein Science*; Wiley Interscience: Hoboken, NJ, 2007; Chapter 2, Unit 2.9.

(34) Lorenzatto, K. R.; Monteiro, K. M.; Paredes, R.; Paludo, G. P.; da Fonsêca, M. M.; Galanti, N.; Zaha, A.; Ferreira, H. B. Fructose-bisphosphate aldolase and enolase from *Echinococcus granulosus*: genes, expression patterns and protein interactions of two potential moonlighting proteins. *Gene* **2012**, *506*, 76−84.

(35) Paredes, R.; Jiménez, V.; Cabrera, G.; Iragüen, D.; Galanti, N. Apoptosis as a possible mechanism of infertility in *Echinococcus granulosus* hydatid cysts. *J. Cell. Biochem.* **2007**, *100*, 1200−9.

(36) Koziol, U.; Krohne, G.; Brehm, K. Anatomy and development of the larval nervous system in *Echinococcus multilocularis*. *Front. Zool.* **2013**, *10*, 24.

(37) Meek, S.; Lane, W.; Piwnica-Worms, H. Comprehensive proteomic analysis of interphase and mitotic 14-3-3-binding proteins. *J. Biol. Chem.* **2004**, *279*, 32046−54.

(38) Keller, A.; Nesvizhskii, A. I.; Kolker, E.; Aebersold, R. Empirical statistical model to estimate the accuracy of peptide identifications made by MS/MS and database search. *Anal. Chem.* **2002**, *74*, 5383−92.

(39) Nesvizhskii, A. I.; Keller, A.; Kolker, E.; Aebersold, R. A statistical model for identifying proteins by tandem mass spectrometry. *Anal. Chem.* **2003**, *75*, 4646−58.

(40) Tatusov, R. L.; Fedorova, N. D.; Jackson, J. D.; Jacobs, A. R.; Kiryutin, B.; Koonin, E. V.; Krylov, D. M.; Mazumder, R.; Mekhedov, S. L.; Nikolskaya, A. N.; Rao, B. S.; Smirnov, S.; Sverdlov, A. V.; Vasudevan, S.; Wolf, Y. I.; Yin, J. J.; Natale, D. A. The COG database: an updated version includes eukaryotes. *BMC Bioinf.* **2003**, *4*, 41.

(41) Powell, S.; Forslund, K.; Szklarczyk, D.; Trachana, K.; Roth, A.; Huerta-Cepas, J.; Gabaldón, T.; Rattei, T.; Creevey, C.; Kuhn, M.; Jensen, L. J.; von Mering, C.; Bork, P. eggNOG v4.0: nested orthology inference across 3686 organisms. *Nucleic Acids Res.* **2014**, *42*, D231−9.

(42) Ferl, R. J.; Manak, M. S.; Reyes, M. F. The 14-3-3s. *Genome Biol.* **2002**, *3*, reviews3010.

(43) Benzinger, A.; Popowicz, G.; Joy, J.; Majumdar, S.; Holak, T.; Hermeking, H. The crystal structure of the non-liganded 14-3-3sigma protein: insights into determinants of isoform specific ligand binding and dimerization. *Cell Res.* **2005**, *15*, 219−27.

(44) Gardino, A.; Smerdon, S.; Yaffe, M. Structural determinants of 14-3-3 binding specificities and regulation of subcellular localization of 14-3-3-ligand complexes: a comparison of the X-ray crystal structures of all human 14-3-3 isoforms. *Semin. Cancer Biol.* **2006**, *16*, 173−82.

(45) Obsil, T.; Obsilova, V. Structural basis of 14-3-3 protein functions. *Semin. Cell Dev. Biol.* **2011**, *22*, 663−72.

(46) Andrade, M.; Siles-Lucas, M.; Espinoza, E.; Pérez Arellano, J.; Gottstein, B.; Muro, A. *Echinococcus multilocularis* laminated-layer components and the E14t 14-3-3 recombinant protein decrease NO production by activated rat macrophages *in vitro*. *Nitric Oxide* **2004**, *10*, 150−5.

(47) Shimada, T.; Fournier, A. E.; Yamagata, K. Neuroprotective function of 14-3-3 proteins in neurodegeneration. *Biomed. Res. Int.* **2013**, *2013*, 564534.

(48) Gygi, S. P.; Corthals, G. L.; Zhang, Y.; Rochon, Y.; Aebersold, R. Evaluation of two-dimensional gel electrophoresis-based proteome analysis technology. *Proc. Natl. Acad. Sci. U.S.A.* **2000**, *97*, 9390−5.

(49) Chang, I. F.; Curran, A.; Woolsey, R.; Quilici, D.; Cushman, J. C.; Mittler, R.; Harmon, A.; Harper, J. F. Proteomic profiling of tandem affinity purified 14-3-3 protein complexes in *Arabidopsis thaliana*. *Proteomics* **2009**, *9*, 2967−85.

(50) Pauly, B.; Lasi, M.; MacKintosh, C.; Morrice, N.; Imhof, A.; Regula, J.; Rudd, S.; David, C. N.; Böttger, A. Proteomic screen in the simple metazoan *Hydra* identifies 14-3-3 binding proteins implicated in cellular metabolism, cytoskeletal organisation and Ca^{2+} signalling. *BMC Cell Biol.* **2007**, *8*, 31.

(51) Alexander, R. D.; Morris, P. C. A proteomic analysis of 14-3-3 binding proteins from developing barley grains. *Proteomics* **2006**, *6*, 1886−96.

(52) Paul, A. L.; Denison, F. C.; Schultz, E. R.; Zupanska, A. K.; Ferl, R. J. 14-3-3 phosphoprotein interaction networks—does isoform diversity present functional interaction specification? *Front. Plant Sci.* **2012**, *3*, 190.

(53) Uhart, M.; Bustos, D. M. Protein intrinsic disorder and network connectivity. The case of 14-3-3 proteins. *Front. Genet.* **2014**, *5*, 10.

(54) Swatek, K. N.; Graham, K.; Agrawal, G. K.; Thelen, J. J. The 14-3-3 isoforms chi and epsilon differentially bind client proteins from developing *Arabidopsis* seed. *J. Proteome Res.* **2011**, *10*, 4076−87.

(55) Kleppe, R.; Martinez, A.; Døskeland, S. O.; Haavik, J. The 14-3-3 proteins in regulation of cellular metabolism. *Semin. Cell Dev. Biol.* **2011**, *22*, 713−9.

(56) Parkinson, J.; Wasmuth, J. D.; Salinas, G.; Bizarro, C. V.; Sanford, C.; Berriman, M.; Ferreira, H. B.; Zaha, A.; Blaxter, M. L.; Maizels, R. M.; Fernández, C. A transcriptomic analysis of *Echinococcus*

DOI: 10.1021/pr5010136
J. Proteome Res. 2015, 14, 1700−1715

granulosus larval stages: implications for parasite biology and host adaptation. *PLoS Negl. Trop. Dis.* **2012**, *6*, e1897.
(57) Chernik, I. S.; Seit-Nebi, A. S.; Marston, S. B.; Gusev, N. B. Small heat shock protein Hsp20 (HspB6) as a partner of 14-3-3gamma. *Mol. Cell. Biochem.* **2007**, *295*, 9−17.
(58) Pan, D.; Das, S.; Bera, A. K.; Bandyopadhyay, S.; De, S.; Rana, T.; Das, S. K.; Suryanaryana, V. V.; Deb, J.; Bhattacharya, D. Molecular and biochemical mining of heat-shock and 14-3-3 proteins in drug-induced protoscolices of *Echinococcus granulosus* and the detection of a candidate gene for anthelmintic resistance. *J. Helminthol.* **2011**, *85*, 196−203.
(59) Jin, J.; Smith, F. D.; Stark, C.; Wells, C. D.; Fawcett, J. P.; Kulkarni, S.; Metalnikov, P.; O'Donnell, P.; Taylor, P.; Taylor, L.; Zougman, A.; Woodgett, J. R.; Langeberg, L. K.; Scott, J. D.; Pawson, T. Proteomic, functional, and domain-based analysis of *in vivo* 14-3-3 binding proteins involved in cytoskeletal regulation and cellular organization. *Curr. Biol.* **2004**, *14*, 1436−50.
(60) Grimm, E.; Portugal, R.; de Oliveira Neto, M.; Martins, N.; Polikarpov, I.; Zaha, A.; Ferreira, H. Structural analysis of an *Echinococcus granulosus* actin-fragmenting protein by small-angle X-ray scattering studies and molecular modeling. *Biophys. J.* **2006**, *90*, 3216−23.
(61) Zhou, Q.; Kee, Y. S.; Poirier, C. C.; Jelinek, C.; Osborne, J.; Divi, S.; Surcel, A.; Will, M. E.; Eggert, U. S.; Müller-Taubenberger, A.; Iglesias, P. A.; Cotter, R. J.; Robinson, D. N. 14-3-3 coordinates microtubules, Rac, and myosin II to control cell mechanics and cytokinesis. *Curr. Biol.* **2010**, *20*, 1881−9.
(62) Gardino, A. K.; Yaffe, M. B. 14-3-3 proteins as signaling integration points for cell cycle control and apoptosis. *Semin. Cell Dev. Biol.* **2011**, *22*, 688−95.
(63) Smith, A. J.; Daut, J.; Schwappach, B. Membrane proteins as 14-3-3 clients in functional regulation and intracellular transport. *Physiology* **2011**, *26*, 181−91.
(64) Dang, Z.; Yagi, K.; Oku, Y.; Kouguchi, H.; Kajino, K.; Watanabe, J.; Matsumoto, J.; Nakao, R.; Wakaguri, H.; Toyoda, A.; Sugimoto, C. Evaluation of *Echinococcus multilocularis* tetraspanins as vaccine candidates against primary alveolar echinococcosis. *Vaccine* **2009**, *27*, 7339−45.
(65) Katoh, Y.; Kouguchi, H.; Matsumoto, J.; Goto, A.; Suzuki, T.; Oku, Y.; Yagi, K. Characterization of emY162 encoding an immunogenic protein cloned from an adult worm-specific cDNA library of *Echinococcus multilocularis*. *Biochim. Biophys. Acta* **2008**, *1780*, 1−6.
(66) Perez-Hernandez, D.; Gutiérrez-Vázquez, C.; Jorge, I.; López-Martín, S.; Ursa, A.; Sánchez-Madrid, F.; Vázquez, J.; Yáñez-Mó, M. The intracellular interactome of tetraspanin-enriched microdomains reveals their function as sorting machineries toward exosomes. *J. Biol. Chem.* **2013**, *288*, 11649−61.
(67) Goc, A.; Abdalla, M.; Al-Azayzih, A.; Somanath, P. R. Rac1 activation driven by 14-3-3ζ dimerization promotes prostate cancer cell-matrix interactions, motility and transendothelial migration. *PLoS One* **2012**, *7*, e40594.

DOI: 10.1021/pr5010136
J. Proteome Res. 2015, 14, 1700−1715